UNIVERSIDADE FEDERAL DE MINAS GERAIS
Programa de Pós-Graduação em Engenharia Metalúrgica, Materiais e de Minas

Tese de Doutorado

DESENVOLVIMENTO DE PROCESSAMENTO POR DEFORMAÇÃO MULTI-AXIAL CÍCLICA E AVALIAÇÃO DO COMPORTAMENTO MECÂNICO E EVOLUÇÃO MICROESTRUTURAL DO ALUMÍNIO

Autor: Natanael Geraldo e Silva Almeida
Orientador: Prof. Dr. Paulo Roberto Cetlin

Maio/2021.

Natanael Geraldo e Silva Almeida

DESENVOLVIMENTO DE PROCESSAMENTO POR DEFORMAÇÃO MULTI-AXIAL CÍCLICA E AVALIAÇÃO DO COMPORTAMENTO MECÂNICO E EVOLUÇÃO MICROESTRUTURAL DO ALUMÍNIO

Tese apresentada ao Programa de Pós-Graduação em Engenharia Metalúrgica, Materiais e de Minas da Escola de Engenharia da Universidade Federal de Minas Gerais, como requisito parcial para obtenção do Grau de Doutor em Engenharia Metalúrgica, Materiais e de Minas.
Área de concentração: Ciência e Engenharia de Materiais
Orientador: Prof. Dr. Paulo Roberto Cetlin.

Belo Horizonte
Universidade Federal de Minas Gerais
Escola de Engenharia
2021

Almeida, Natanael Geraldo e Silva.
A447d Desenvolvimento de processamento por deformação multi-axial cíclica e avaliação do comportamento mecânico e evolução microestrutural do alumínio [recurso eletrônico] / Natanael Geraldo e Silva Almeida. - 2021.
1 recurso online (58 f. : il., color.) : pdf.

Orientador: Paulo Roberto Cetlin.

Tese (doutorado) - Universidade Federal de Minas Gerais, Escola de Engenharia.

Inclui bibliografia.
Exigências do sistema: Adobe Acrobat Reader.

1. Materiais - Teses. 2. Ciência dos materiais - Teses. 3. Alumínio - Teses. 4. Metais - Deformação - Teses. I. Cetlin, Paulo Roberto, 1946-. II. Universidade Federal de Minas Gerais. Escola de Engenharia. III. Título.

CDU: 620(043)

Ficha catalográfica elaborada pelo bibliotecário Reginaldo Cesar Vital dos Santos, CRB/6 2165
Biblioteca Prof. Mário Werneck, Escola de Engenharia da UFMG

UNIVERSIDADE FEDERAL DE MINAS GERAIS
ESCOLA DE ENGENHARIA
Programa de Pós-Graduação em Engenharia Metalúrgica, Materiais e de Minas

Tese intitulada **"Desenvolvimento de Processamento Por Deformação Multi-axial Cíclica e Avaliação do Comportamento Mecânico e Evolução Microestrutural do Alumínio"**, área de concentração: Ciência e Engenharia de Materiais, apresentada pelo candidato **Natanael Geraldo e Silva Almeida**, para obtenção do grau de Doutor em Engenharia Metalúrgica, Materiais e de Minas, aprovada pela comissão examinadora constituída pelos seguintes membros:

Prof. Paulo Roberto Cetlin
Orientador - Dr. (UFMG)

Profª Elaine Carballo Siqueira Corrêa
Drª (CEFET/MG)

Prof. Pedro Henrique Rodrigues Pereira
Dr. (UFMG)

Prof. Wellington Lopes
Dr. (CEFET/MG)

Prof. Cleber Granato de Faria
Dr. (Newton Paiva)

Profª Maria Teresa Paulino Aguilar
Drª (UFMG)

Prof. Rodrigo Lambert Oréfice
Coordenador do Programa de Pós-Graduação em Engenharia Metalúrgica, Materiais e de Minas/UFMG

Belo Horizonte, 13 de maio de 2021

Sumário

RESUMO

A constante busca por metais com propriedades mecânicas cada vez mais atrativas leva ao desenvolvimento de novas técnicas de processamento. Processos de fabricação que envolvem deformação plástica severa (*Severe Plastic Deformation* – SPD) tem sido amplamente utilizados com o objetivo de aumentar a resistência mecânica dos metais. Estas técnicas promovem o refino do tamanho de grão à escala submicrométrica de forma a aumentar a resistência mecânica dos metais. Dentre as técnicas de SPD, o processamento por MDF (*Multi Directional Forging*) se destaca por ser: (i) a única técnica de deformação plástica severa que permite acompanhar a curva tensão x deformação durante o processamento; (ii) um processamento simples, podendo ser realizado em qualquer equipamento de compressão, até mesmo sem ferramental específico e (iii) possibilitar o processamento de peças com grandes dimensões. As metodologias adotadas para o processamento por MDF geram dificuldades durante o processamento devido às distorções geométricas causadas pelo atrito entre o material e as superfícies de compressão, o que dificulta o controle do processo. As alternativas para resolver estes problemas aumentam o tempo e custo de processamento ou alteram o caminho de deformação e, consequentemente, as propriedades finais do material processado. Este trabalho tem o objetivo de desenvolver uma metodologia de processamento por MDF que elimine as dificuldades atuais e comparar os resultados obtidos por esta metodologia e as demais metodologias que utilizam o estado triplo de deformação empregando o alumínio como exemplo de material. A metodologia desenvolvida é eficiente, reduz o tempo de processamento, apresenta menor custo, mantém o estado triplo de deformação e elimina os maiores problemas encontrados nas metodologias presentes na literatura. A distribuição de deformação, microdureza e evolução microestrutural apontam para uma maior deformação na região central das amostras quando comparada com as extremidades.

Palavras chave: Deformação Pástica Severa, MDF, alumínio.

ABSTRACT

The constant search for metals with outstanding mechanical behavior leads to the development of new processing techniques. Manufacturing processes that involve severe plastic deformation (SPD) have been widely used to improve the mechanical behavior of metals. These techniques promote the grain size refinement on a submicron scale in order to increase the metal strength. Among SPD techniques, MDF (Multi Directional Forging) stands out for the following advantages: (i) it is the only severe plastic deformation technique that allows the determination of the stress x strain curves for the material during processing, (ii); it is a simple processing technique that can be performed on any compression equipment, even without special tools and (iii) it allows the processing of large samples. The methodologies adopted for MDF processing present some difficulties during processing due to geometric distortions caused by the friction between the material and the compression tools. Those problems make it difficult to control the process. The alternatives to solve those problems increase the processing time and cost or change the strain path, and consequently the final properties of the processed material. This work aims to develop an MDF processing methodology that eliminates the current difficulties as well as to compare the results obtained by this methodology and the other methodologies that use the triaxial strain state, for the specific case of Aluminum processing. The developed methodology is efficient, decreases the processing time, is cheaper, maintains the triaxial strain state, and eliminates the main problems found in the literature's methodologies. The strain distribution, microhardness, and microstructural evolution point to a greater deformation in the central region of the samples when compared with the extremities.

Key words: Severe Plastic Deformation, MDF, aluminum.

ESTRUTURA DA TESE

Esta tese está organizada em capítulos.

O capítulo 1 contém a contextualização do tema, motivação, e originalidade, bem como os objetivos e a descrição do material e métodos adotados.

Nos capítulos 2 e 3 são apresentados os dois artigos publicados com os resultados obtidos neste trabalho. Para facilitar a leitura, não foi adotada a formatação original publicada pelas revistas.

Os capítulos 4 e 5 apresentam, respectivamente, as conclusões e sugestões para trabalhos futuros.

1 INTRODUÇÃO

1.1 CONTEXTUALIZAÇÃO, MOTIVAÇÃO E ORIGINALIDADE

A constante busca por metais com propriedades mecânicas cada vez mais atrativas leva ao desenvolvimento de novas técnicas de processamento. Neste contexto, materiais como o alumínio e suas ligas são de grande interesse devido a sua boa ductilidade, acabamento atrativo e capacidade de se combinar com a maioria dos metais de engenharia, além de baixo custo e peso específico, resistência à corrosão, boa condutividade térmica e elétrica [1].

Processos de fabricação que envolvem deformação plástica severa (*Severe Plastic Deformation* – SPD) têm sido amplamente utilizados com o objetivo de aumento de resistência mecânica de metais. Estes processos utilizam métodos em que o material metálico é deformado plasticamente até elevadas quantidades de deformação sem alterações apreciáveis nas dimensões e forma iniciais do material. O objetivo da técnica é refinar o tamanho de grão à escala submicrométrica de forma a aumentar a resistência mecânica do metal (segundo a equação de Hall-Petch). Dentre as técnicas de SPD, as mais estudadas na literatura são: Torção sob Elevada Pressão (*High Pressure Torsion*- HPT) [2], União por Laminação Acumulativa (*Accumulative Roll-Bonding*, ARB) [3], Extrusão Angular em Canais Iguais (*Equal Channel Angular Pressing*, ECAP) [4] e Forjamento Multi-Axial (*Multi Directional Forging* – MDF) [5-7].

O processamento por MDF (*Multi Directional Forging*) ou MAC (*Multi Axial Compression*), como também é conhecido, consiste em promover compressões sequenciais alternando a direção na qual é aplicada a deformação [5], conforme ilustrado na Figura 1.1.

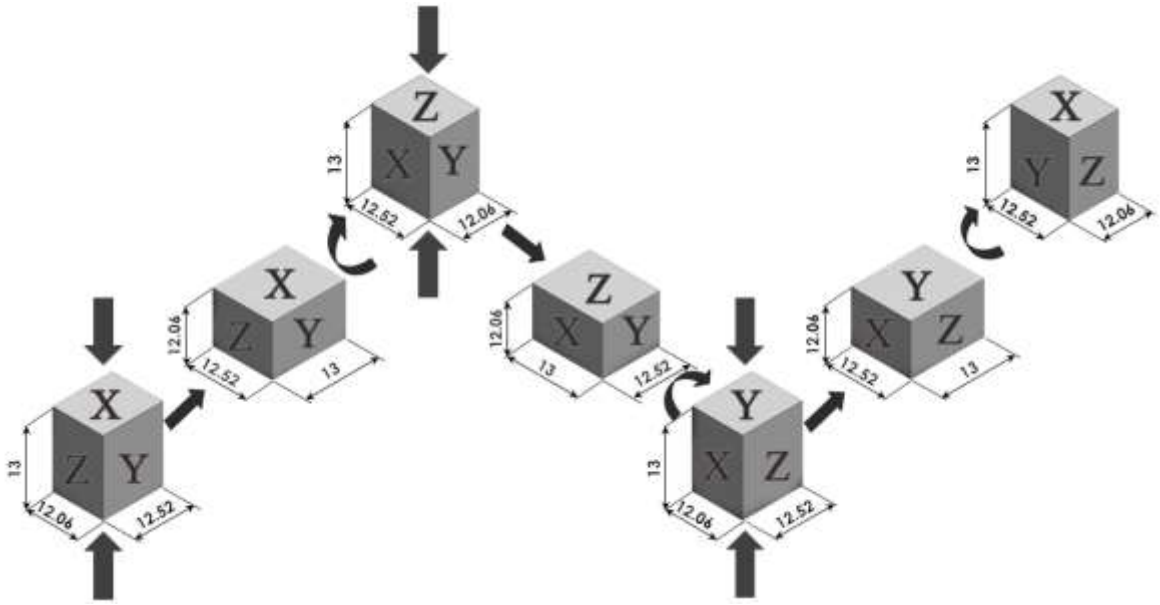

FIGURA 1.1 – Representação esquemática do processo de compressão multiaxial [8].

Quando comparada às demais técnicas de processamento por SPD, o processamento por MDF apresenta as seguintes vantagens: é a única técnica de deformação plástica severa que permite acompanhar a curva tensão x deformação durante o processamento; é um processamento simples, podendo ser realizado em qualquer equipamento de compressão, até mesmo sem ferramental específico e é possível ser adotado em peças com grandes dimensões [6].

No início da deformação por MDF se obtêm grãos alongados, além de ocasionar o aumento da densidade de deslocações. Com o aumento da quantidade de deformação os grãos vão assumindo um formato mais próximo de equiaxial [9]. Além disso, com o aumento da deformação se obtêm uma estrutura com contornos de alto ângulo e menor densidade de deslocações, o que pode conduzir ao amaciamento [10]. Materiais pré-deformados podem ter seu comportamento mecânico aprimorado quando submetidos ao MDF; com destaque para a possibilidade de processamento de matérias frágeis, atuando no progressivo refino de grãos [5].

O MDF pode ser utilizado em combinações de processamento; combinando-o com compressões uniaxiais [11], e até mesmo com outros processos SPD, como o ECAP, que consiste em forçar a passagem de uma amostra maciça por dois canais, com seção transversal iguais, angulados entre si [6]. O processamento por MDF no material processado por ECAP regenera parcialmente a ductilidade perdida [8,12-13]. O ECAP atua na formação de células no interior dos grãos pré-existentes e o MDF, por sua vez, atua promovendo o aumento na desorientação entre os grãos e

a diminuição da densidade de deslocações nas regiões internas destes grãos. Ademais, a estrutura de deslocações tende a se estabilizar com o processamento por MDF [14].

Após a primeira compressão do processamento por MDF, realizado somente com o auxílio das placas planas de compressão, a amostra assume uma forma abaulada, ou seja, suas laterais ficam arredondadas. Isso ocorre devido às forças de atrito entre as superfícies da amostra que tocam as bases de compressão, que dificultam a deformação das regiões da amostra mais próximas aos contatos. Com isso, para as próximas compressões não se tem mais faces planas, tão pouco paralelas, a serem comprimidas (Fig. 1.2). Essas distorções geométricas das faces a serem comprimidas geram alterações no início da curva tensão x deformação, que não mais representaria somente o comportamento do material. Além disso, superfícies irregulares das faces a serem comprimidas dificultam o posicionamento da amostra, uma vez que é difícil equilibrar o corpo de prova tendo como base de aóio uma face abaulada e ainda conseguir garantir o alinhamento com a direção de deformação, conforme ilustrado na Figura 1.2. Finalmente, quando se tem faces irregulares se torna complicado garantir a imposição de uma quantidade de deformação específica [7,11,13,15].

Para eliminar estes problemas, é possível realizar a usinagem das faces abauladas após cada compressão. Esta usinagem elimina os problemas de posicionamento da amostra para a sequência de compressões, elimina os problemas de distorção na curva que representa o comportamento mecânico e garante a precisão da quantidade de deformação obtida em cada compressão [11,16,17]. Porém, essas usinagens são demoradas e caras. Algumas pesquisas utilizam matrizes que restringem a deformação da próxima direção a ser comprimida, o que elimina os problemas supracitados, porém, altera o caminho de deformação devido a imposição do estado plano de deformação [18-23]. Este trabalho desenvolveu uma metodologia para o processamento por MDF que elimine os problemas citados mantendo o estado triplo de deformação e comparar os resultados obtidos por esta metodologia e as demais que envolvem triaxialidade de deformação, através da análise da evolução do comportamento mecânico e microestrutural, para o caso específico do processamento do Alumínio.

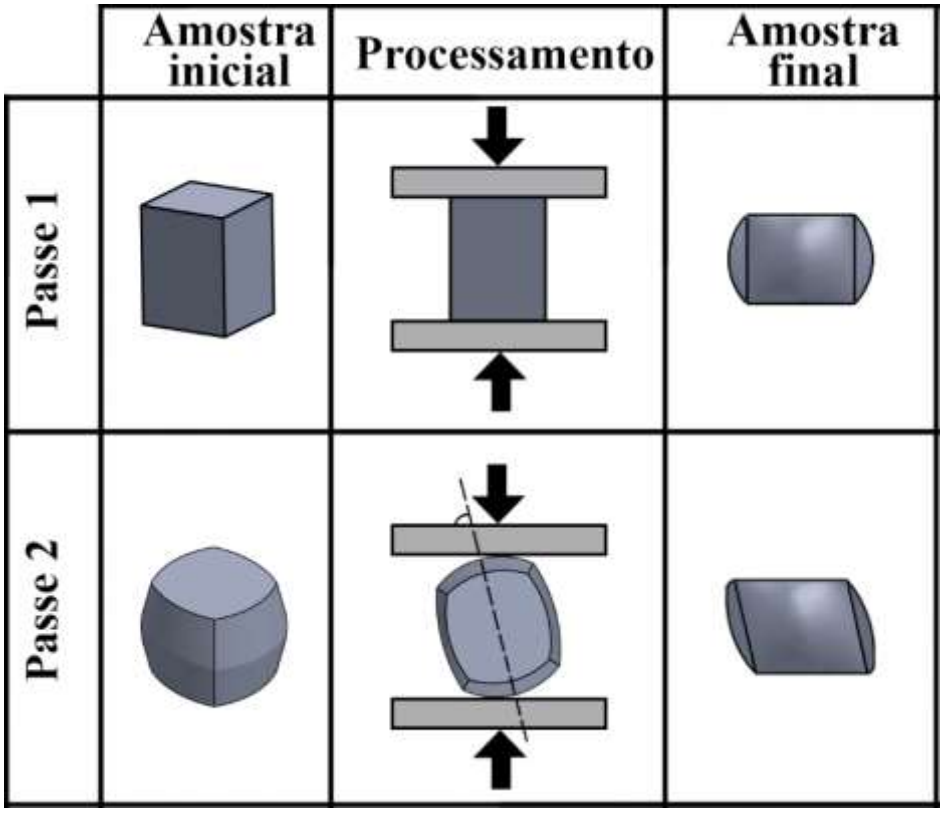

Figura 1.2 – Representação esquemática do primeiro e segundo passe do processamento por MDF.

O tema deste doutoramento surgiu com o desenvolvimento de pesquisas relacionadas a processamentos SPD e à caracterização mecânica e microestrutural do alumínio processado por estas técnicas. Estes trabalhos prévios serviram de referência paro o estudo atual, de forma indireta por meio do envolvimento com o tema e de forma direta por meio da comparação dos dados. Os resultados destas pesquisas foram utilizados para a publicação da dissertação *"Comportamento mecânico da liga Al 6351 submetida à extrusão angular em canais iguais e compressão multiaxial cíclica"* [8] e os seguintes artigos: *"Increasing the work hardening capacity of equal channel angular pressed (ECAPed) aluminum through multi-axial compression (MAC)"* [13], *"Microstructural evolution in the low strain amplitude multi-axial compression (LSA-MAC) after equal channel equal pressing (ECAP) of aluminum"* [14], *"Mechanical behavior and microstructures of aluminum in the Multi-Axial Compression (MAC) with and without specimen re-machining"* [15], *"The effect of initial strain in the severe plastic deformation of Aluminum on the subsequent work hardening regeneration through Low Strain Amplitude Multi-Directional Forging"* [24] e *"The Design of a Die for the Processing of Aluminum through Equal Channel Angular Pressing"* [25].

1.2 OBJETIVOS

Desenvolver uma metodologia de processamento por MDF que elimine os problemas e as dificuldades das metodologias adotadas comumente e comparar os resultados obtidos com esta nova metodologia e as demais através da análise do comportamento mecânico e a evolução microestrutural do alumínio.

Para isso os seguintes objetivos específicos foram atingidos:

1- Desenvolvimento de uma metodologia para a realização do processamento por MDF, em estado triplo de deformação, que elimine os problemas encontrados nas metodologias atuais;

2- projeto e fabricação de uma ferramenta capaz de executar a metodologia idealizada de forma eficiente;

3- comparação do comportamento mecânico e evolução da microestrutura do processamento do alumínio comercialmente puro processado pela metodologia desenvolvida e as principais metodologias encontradas na literatura.

1.3 MATERIAL E MÉTODOS

O material utilizado foi o Alumínio comercialmente puro (99,77% Al, 0,15% Fe, 0,06 Si) recebido no estado bruto de fusão, o estudo seguiu o fluxograma ilustrado na Figura 1.3. O material foi processado por ECAP, com o objetivo de quebrar a estrutura bruta de fusão, e recozido a 400 ºC por 1 hora. Para a realização do MDF sem a necessidade de usinar as amostras a cada passe, foi projetada e fabricada uma matriz que permitisse o processamento mantendo a triaxialidade de deformação. Após o processamento das amostras, estas foram analisadas por EBSD (*Electron BackScattered Diffraction*) e TEM (*Transmission Electron Microscopy)* após 1 e 4 ciclos de MDF com amplitude de deformação igual a 0.075. Os resultados obtidos por estas análises foram utilizados na publicação do artigo I: *"Mechanical behavior and microestructures of aluminum processed by low strain amplitude multi-directional confined forging"*. Além do processamento das amostras de Alumínio pela metodologia desenvolvida, novas amostras foram processadas sem o auxílio da matriz com e sem usinagem entre as compressões. Todas as amostras processadas foram mapeadas através de medições de microdureza Vickers. Simulações numéricas foram realizadas pelo método dos elementos finitos (*Finite Element Method* – FEM) para cada condição de processamento, com o objetivo de avaliar a distribuição de deformação envolvida em cada metodologia. Além disso, a evolução microestrutural destas amostras foi avaliada por microscopia óptica e EBSD. Estes resultados foram utilizados para a publicação do artigo II: *"Hardness, Microstructure and Strain Distributions in Commercial Purity Aluminum Processed by Multi Directional Forging (MDF)"*.

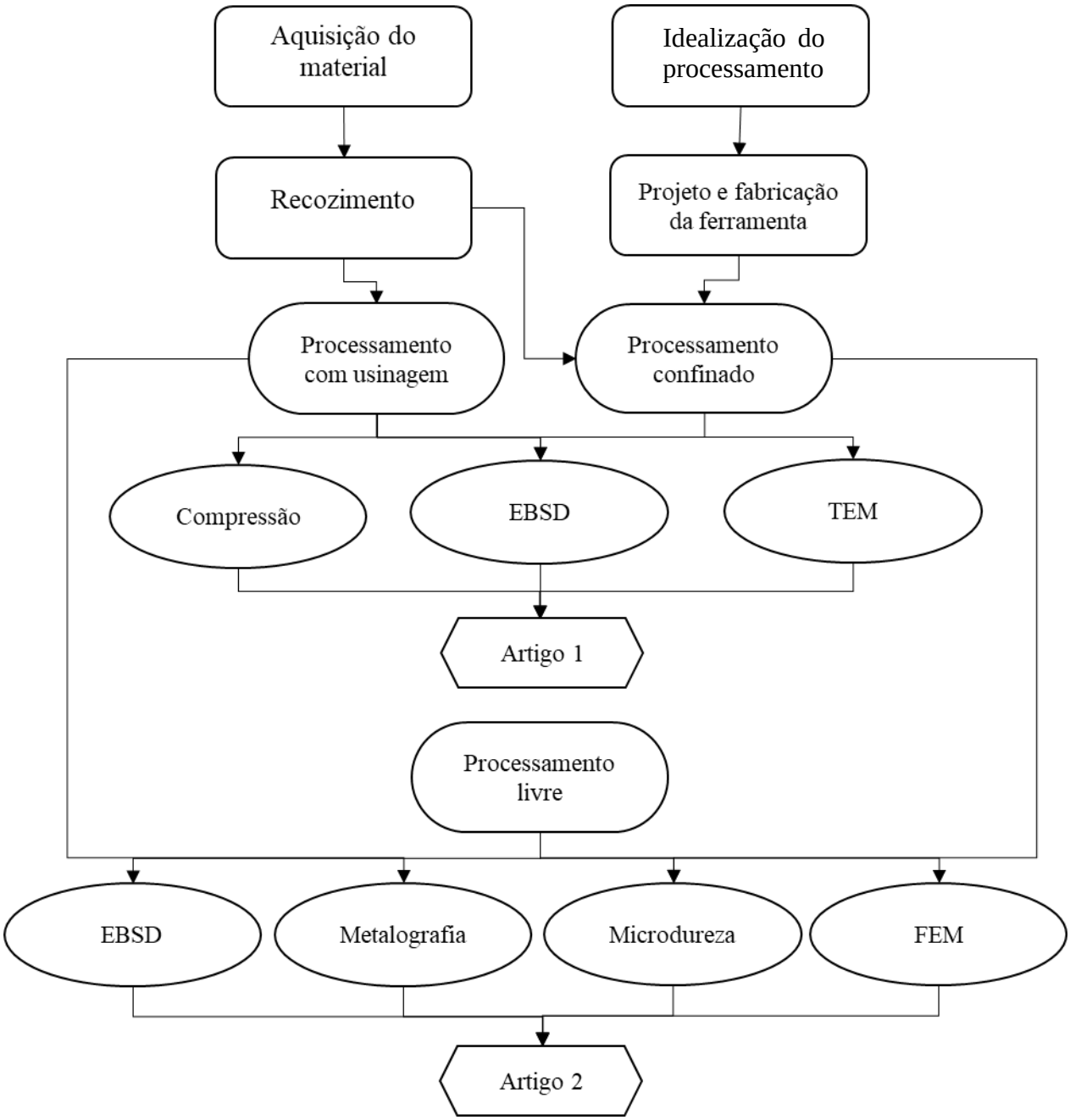

Figura 1.3 – Fluxograma do planejamento experimental

1.4 REFERÊNCIAS BIBLIOGRÁFICA

[1] ASM INTERNATIONAL. ASM Handbook. Properties and selection: Nonferrous alloys and special-purpose materials. 10 ed. Ohio: American Society for Metals - ASM international, v. 2, 1990.

[2] ZHILYAEV, A. P.; LANGDON, T. G. Using high-pressure torsion for metal processing: fundamentals and applications. Progress in Materials Science. v. 53, p. 893-979, 2008.

[3] SAITO, Y.; TSUJI, N.; UTSUNOMIYA, H.; SAKAI, T.; HONG, R. G. Ultra fine grained bulk aluminum produced by accumulative roll-bonding (ARB) process. Scripta Materialia. v. 39, n. 9, p. 1221-1227, 1998.

[4] VALIEV, R. Z.; LANGDON T.G. Principles of equal-channel angular pressing as a processing tool for grain refinement. Progress in Materials Science. v. 51, p. 881-981, 2006.

[5] VALIEV, R. Z.; ISLAMGALIEV R. K.; ALEXANDROV, I. V. Bulk nanostructured materials from severe plastic deformation. Progress in Materials Science. v. 45, p. 103-189, 2000.

[6] SAKAI, T.; BELYAKOV, A.; KAIBYSHEV, R.; MIURA, H.; JONAS, J. J. Dynamic and post-dynamic recrystallization under hot, cold and severe plastic deformation conditions. Progress in Materials Science. v. 60, p. 130-207, 2014.

[7] ZHU, Q.; LI, L.; BAN, C.; ZHAO, Z.; ZUO, Y.; CUI, J., Structure uniformity and limits of grain refinement of high purity aluminum during multi-directional forging process at room temperature. Transactions of Nonferrous Metals Society of China. v. 24, p. 1301-1306, 2014.

[8] ALMEIDA, N. G. S. Comportamento mecânico da liga Al 6351 submetida à extrusão angular em canais iguais e compressão multiaxial cíclica. Belo Horizonte: Escola de Engenharia da UFMG, 2017. 90p (Dissertação, Mestrado em Engenharia Mecânica).

[9] YANG, X.; WANG, D.; WU, Z.; YI, J.; NI, S.; DU, Y. A coupled EBSD/TEM study of the microstructural evolution of multiaxial compressed pure Al and Al–Mg alloy. Materials Science & Engeneering A. v. 658, p 16-27, 2016.

[10] KAPOOR, R.; SARKAR, A.; YOGI, R.; SHEKHAWAT, S. K.; SAMAJDAR, I; CHAKRAVARTTY, J. K. Softening of Al during multi-axial forging in a channel die. Materials Science & Engeneering A. v. 560, p. 404-412, 2013.

[11] ARMSTRONG, P. E; HOCKETT, J. E.; SHERBY, O. D. Large strain multidirectional deformation of 1100 aluminum at 33K. Journal of the Mechanics and Physics of Solids. v. 30, n. 1/2, p. 37-58, 1982.

[12] FARIA, C. G. Processamento multiaxial cíclico em alumínio comercialmente puro processado por ECAP. Belo Horizonte: Escola de Engenharia da UFMG, 2015. 85p (Dissertação, Mestrado em Engenharia Mecânica).

[13] FARIA, C. G.; ALMEIDA, N. G. S.; AGUILAR, M. T. P.; CETLIN, P. R. Increasing the work hardening capacity of equal channel angular pressed (ECAPed) aluminum through multi-axial compression (MAC). Materials Letters. v. 174, p. 153-156, 2016.

[14] FARIA, C. G.; ALMEIDA, N. G. S.; BUBANI, F. C.; BALZUWEIT, K.; AGUILAR, M. T. P.; CETLIN, P. R. Microstructural evolution in the low strain amplitude multi-axial compression (LSA-MAC) after equal channel equal pressing (ECAP) of aluminum. Materials Letters. v, 227, p. 149-53, 2018.

[15] STEMLER, P. M.; FLAUSINO, P. C.; PEREIRA, P.H.; DE FARIA, C. G.; ALMEIDA, N. G.; AGUILAR, M. T. P.; CETLIN, P. R. Mechanical behavior and microstructures of aluminum in the Multi-Axial Compression (MAC) with and without specimen re-machining. Materials Letters. v. 237, p. 84-7, 2019.

[15] LI YJ, BLUM W. Strain rate sensitivity of Cu after severe plastic deformation by multiple compression. Physica Status Solidi. v. 202, p. 119-21, 2005.

[16] LI, Y. J.; ZENG, X, H,; BLUM, W. On the elevated-temperature deformation behavior of polycrystalline Cu subjected to pre deformation by multiple compression. Materials Science and Engineering A. v. 483, p. 547-50, 2008.

[17] KUMAR, S. S. S.; RAGHU, T. Bulk processing of fine grained OFHC copper by cyclic channel die compression. International Journal of Materials Research. v. 106, p. 1230–9, 2015.

[18] BERGHAMMER, R.; HU, W.; HASANI, A. Gottstein G. Production of Ultrafine Grained AlMnFe Samples by Confined Channel Die Pressing as Compared to Equal Channel Angular Pressing. Advanced Engineering Materials. v. 13, p. 232-6, 2011.

[19] KAPOOR, R.; SARKAR, A.; YOGI, R.; SHEKHAWAT, S. K.; SAMAJDAR, I; CHAKRAVARTTY, J. K. Softening of Al during multi-axial forging in a channel die. Materials Science & Engeneering A. v. 560, p. 404-412, 2013.

[20] ZHAO, S.; MENG, C.; MAO, F.; HU, W. Influence of severe plastic deformation on dynamic strain aging of ultrafine grained Al–Mg alloys. Acta Materialia. v. 76, p. 54 – 67, 2014.

[21] ZHANG, S.; HU, W.; BERGHAMMER, R.; GOTTSTEIN, G. Microstructure evolution and deformation behavior of ultrafine-grained Al–Zn–Mg alloys with fine η′ precipitates. Acta Materialia. v. 58(60), p. 6695-705, 2010.

[22] LIU, G.; GU, J.; NI, S.; LIU, Y, SONG, M. Microstructural evolution of Cu–Al alloys subjected to multi-axial compression. Materials Characterization. v. 103, p. 107-119, 2015.

[23] MU, S. J.; HU, W. P.; GOTTSTEIN, G. Investigations on Deformation Behavior and Microstructure of Ultrafine Grained Two Phase Al-Mn Alloy Fabricated by Confined Channel Die Pressing. Materials Science Forum. v. 584-586: p. 697-702, 2008.

[24] FARIA, C. G.; ALMEIDA, N. G. S.; BUBANI, F. C.; BALZUWEIT, K.; AGUILAR, M. T. P.; CETLIN, P. R. The effect of initial strain in the severe plastic

deformation of Aluminum on the subsequent work hardening regeneration through Low Strain Amplitude Multi-Directional Forging. Materials Letters. v, 290, p. 01-05, 2021.

[25] P. G. F. SIQUEIRA, N. G. S. ALMEIDA, P. M. A. STEMLER, P. R. CETLIN, M. T. P. AGUILAR. The Design of a Die for the Processing of Aluminum through Equal Channel Angular Pressing. World Academy of Science, Engineering and Technology International Journal of Materials and Metallurgical Engineering. v. 4: p. 97- 100, 2020.

2 ARTIGO I

2.1 TITLE AND ABSTRACT

MECHANICAL BEHAVIOR AND MICROSTRUCTURES OF ALUMINUM PROCESSED BY LOW STRAIN AMPLITUDE MULTI-DIRECTIONAL CONFINED FORGING

Severe Plastic Deformation (SPD) leads to grain refinement and strengthening of metals. Among many SPD processing methods, Multi-Directional Forging (MDF) is the only one where in-situ material stress-strain curves can be obtained. These are adequate only for specimens re-machined after each compression step, thus avoiding problems connected to specimen shape distortions; re-machining involves complex, expensive and time consuming procedures. This difficulty has been circumvented using confined plane strain compressions, where the strain path, however, differs from that in simple, unconfined free compression. A new processing method involving, for each processing step, an initial free simple compression followed by a confined compression (Multi-Directional Confined Forging – MDCF) is proposed, eliminating the specimen re-machining. Strengthening by MDF depends on strain amplitude; low strain amplitude MDF (LSA-MDF) leads to lower work hardening of the material than high strain amplitude MDF, as well as to limited softening and to an increase in the residual work hardening capacity of material previously deformed monotonically or in successive deformation steps with high strain amplitudes. This supplies a highly desired enhanced uniform elongation of the material after SPD. It is shown that Low Strain Amplitude Multi-Directional Confined Forging (LSA-MDCF) of Aluminum leads to adequate stress-strain curves up to the contact of the specimen with the confining die walls, as well as to microstructures very similar to those obtained using free compressions with re-machined specimens. This processing route is simpler, faster and cheaper than LSA-MDF with re-machined samples, and thus emerges as a more practical MDF route.

Keywords: Aluminum; Microstructures; Multi-Directional Forging; Severe plastic deformation; Stress-strain curves.

2.2 INTRODUCTION

Severe Plastic Deformation (SPD) of metals has been widely studied in the last decades as an efficient method for their grain refinement and strengthening, without appreciable changes in the original dimensions of the workpieces. The most utilized SPD techniques are Equal Channel Angular Pressing (ECAP) [1], High Pressure Torsion (HPT) [2], and Multi-Directional Forging (MDF), also known as Multi-Axial Compression (MAC) or Multi-Axial Forging (MAF) [3-5]. In addition to the above mentioned strengthening, SPD is important in the micro-forming of components [6-8] and in the superplastic forming of metals, which can then be performed under increased strain rates, enhancing the economic aspects of this type of processing [9].

Sakai et al. [3] consider that MDF has the following advantages over other SPD techniques: (i) it is the only SPD method where in-situ stress-strain curves of the material (hereafter denominated SS curves) can be reliably obtained for each compression step during processing, (ii) the testing procedure is simple, can use any conventional testing machine or industrial press, at various temperatures and strain rates and (iii) can be applied to large industrial workpieces.

MDF with simple free compression leads to specimen distortions [10,11] and inadequate SS curves [12,13]; in addition, the irregular shapes of the specimens cause severe strain heterogeneities in the material [11, 14] and difficulties in the measurement of the specimen instantaneous dimensions [13]. These problems have been circumvented by re-machining the specimens after each compression or after a few compressions [10,15,16], which is complicated, expensive and time consuming. A solution to these difficulties involves processing the material under plane strain with confining dies [17, 18]. The confinement has been used in only one direction normal to the compression direction and along the plane strain direction (the so-called CCDC: Confined Channel Die Compression) [17, 18] or in both directions normal to the compression (the so-called CCDP: Confined Channel Die Pressing) [19-24]. Comparisons of the mechanical behavior of the material under simple free compression and under plane strain compression are complex, since their strain paths differ [25].

The strain amplitude employed in MDF has a fundamental influence on the flow behavior of the material, as initially described by Armstrong *et al*. [10]. As this amplitude is lowered the work hardening rate of the material decreases together with the resulting saturation stress level. These authors showed that this is also valid for the strain amplitudes utilized for deformation under cyclic tension-compression and reversed torsion in aluminum, copper and steel. Low strain amplitude MDF (LSA-MDF) involves an excessive number of compression steps necessary to achieve the adequate levels of strain and thus is not practical and economical. On the other hand, LSA-MDF after monotonic deformation causes a limited work softening of the material associated with a pronounced gain in the work hardening rate under further monotonic deformation, with a consequent increase in the material uniform elongation under tensile testing. The present authors submitted commercial purity Aluminum to one ECAP pass, imposing a monotonic strain ≈ 1.15, and then applied on the material 12 LSA-MDF free compressions with strain amplitude 0.075 [12]. Monotonic compression of the material after ECAP + LSA MDF showed that there was a limited decrease in the yield strength of the material and an increase in its work hardening capacity, when compared with the behavior of the material compressed directly after ECAP. Since MDF does not alter the geometry of the material, it was thus possible to produce material with a high strength and enhanced uniform elongation, caused by the now increased work hardening capacity.

From the point of view of the material microstructure, it has been shown that MDF leads initially to an increase in the dislocation density, involving tangled structures. As straining proceeds, a cellular structure is established with an increasing proportion of Low Angle Grain Boundaries (LAGBs); further straining by MDF causes the evolution of these LAGBs into High Angle Grain Boundaries (HAGBs), associated with dynamic recovery phenomena. This deformation stage may cause work softening of the material [20]. As the strain amplitude is lowered, this structure evolution is retarded and the dislocation structures at LAGBs and HAGBs often remain diffuse [26]. The application of LSA-MDF after monotonic deformation or after successive high strain amplitude deformations leads to a destabilization of the initially prevailing dislocation

structure, which tends to an arrangement that would exist in case only LSA-MDF had been utilized [27].

This investigation presents a new LSA-MDF processing technique, wherein the compression occurs inside a prismatic confining die, and the material is allowed to expand sideways in all directions normal to the compression direction till reaching the die walls (the so-called LSA-MDCF – Low Strain Amplitude Multi-Directional Confined Forging). The in-situ SS curves of the material and the dislocation structures resulting from the use of this technique are analyzed. A comparison of these results with those obtained for LSA-MDF under free-compression with re-machined specimens [13] is also presented.

2.3 EXPERIMENTAL PROCEDURE

Billets of cast aluminum (99.77%) were initially processed as described in previous investigations [13]. LSA-MDCF specimens with dimensions 13.00 x 12.52 x 12.06 mm (along the initial X, Z and Y axes in Figure 2.1, respectively) were machined out of the annealed material. A tool steel die having an internal rectangular cross-section of 13.00 x 12.52 mm, as schematically shown in Figure 2.1, was designed for LSA-MDCF with a strain amplitude $\Delta\varepsilon = 0.075$. Other dimensions of specimens and dies can obviously be adapted to any specimen size and strain amplitude.

Specimens were put into the die with their largest dimension (13.00 mm) aligned with the compression direction, and then upset down to 12.06 mm ($\varepsilon = 0.075$). Their lateral dimensions evolved from 12.52 to 13.00 mm ($\varepsilon = 0.0375$) and from 12.06 to 12.52 mm ($\varepsilon = 0.0375$) according to the restrictions of the confining die. The lower die was removed, and further punch movement extracted the specimen, which was then rotated and re-inserted into the die so that the new 13.00 mm dimension lied in the compression direction and so successively. After each three multi-directional three compressions (a so called “LSA-MDCF cycle”), the specimen returned to its original dimensions along the X, Z and Y axes. An illustration of the procedure is given elsewhere [12]. Four LSA-MDCF cycles were performed (12 compressions, totaling a

Von Mises equivalent strain of 0.9); further processing could obviously be carried on to any number of cycles and strain amplitudes, up to an eventual fracture of the material. In order to determine the true stress-true strain curves for the material from

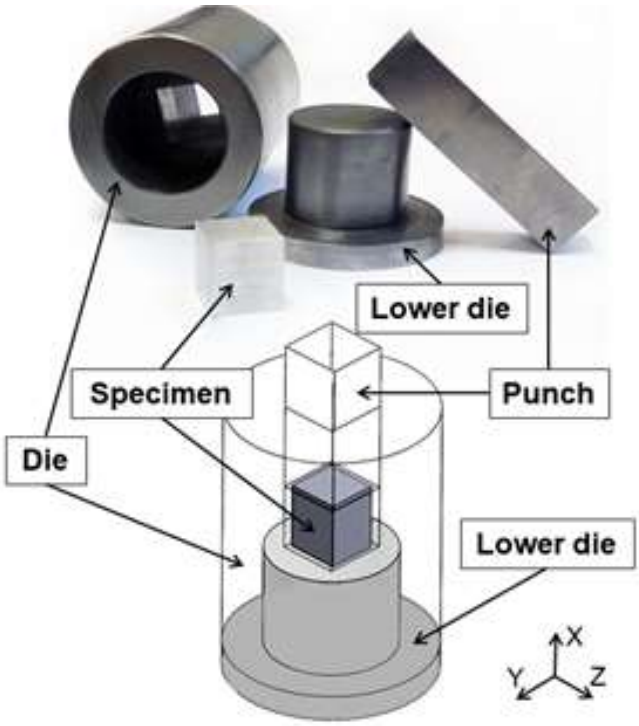

Figure 2.1 – Schematic illustration and photographs of the LSA-MDCF die and the Al specimen.

the load – punch displacement experimentally determined curves, the following procedures were adopted: (i) specimens were submitted to increasing loads and the height of the specimen was measured after unloading, till the specimen reached the desired final height (from 13.00 mm down to 11.06 mm, with a height reduction of 1.94 mm); (ii) the punch displacement at the applied load for the specimen height of 11.06 mm was measured; (iii) the difference between this displacement and the specimen change of height (1.94 mm) was calculated, and the applied load was divided by this difference for the determination of the system's elastic compliance; (iv) a series of loads were taken along the load vs punch displacement curves, and the elastic component of the punch displacement was calculated using the system's compliance; (v) the instantaneous plastic decrease in height of the specimen was calculated

subtracting this elastic component from the total punch displacement; (vi) the instantaneous height of the specimen was calculated subtracting this plastic decrease of height from the specimen initial height (vii) ; the instantaneous average cross-sectional area of the specimen was calculated dividing the specimen volume by its instantaneous height; (viii) true stress was then calculated as the instantaneous load divided by the instantaneous cross-sectional area, and true strain was calculated based on the specimen initial and instantaneous height. Processing occurred at room temperature using an INSTRON 5582 machine and a crosshead speed ~ 0.05 mm/s. No notable differences were observed for duplicate experiments.

Studies in the literature report that the maximum strain in specimens processed by MDF occur in the center of the specimen [19, 28, 29]. The microstructures in this region for LSA-MDCF specimens processed up to 1 and 4 cycles were thus examined through Electron Back-Scattered Diffraction (EBSD) and Transmission Electron Microscopy (TEM) using the same experimental procedures described in an earlier investigation [27]. EBSD scans and TEM analyses were also performed in aluminum specimens previously processed through LSA-MDF without die confinement, in order to compare its microstructure with that obtained through LSA-MDCF [13]. It should be noted that these Al samples were periodically re-machined avoiding the deleterious effects associated with the onset of excessive material distortion during processing.

2.4 RESULTS AND DISCUSSION

Figure 2.2 shows the experimental SS curves for the 4 LSA-MDCF cycles with a strain amplitude $\Delta\varepsilon = 0.075$. Each SS curve is designated by a letter (X, Z or Y) corresponding to the compression direction, and a number (1, 2, 3 or 4) corresponding to the LSA-MDCF cycle. All curves in Figure 2.2 display increasingly positive slopes in their final regions. Careful examination of the specimens along interrupted compressions in several of the processing steps revealed that the beginning of this slope increment corresponds to the contact of the laterally expanding specimen with the die walls. These walls restrict the plastic flow and impose a triaxial state of stresses on the specimen which ultimately leads to increased applied stresses.

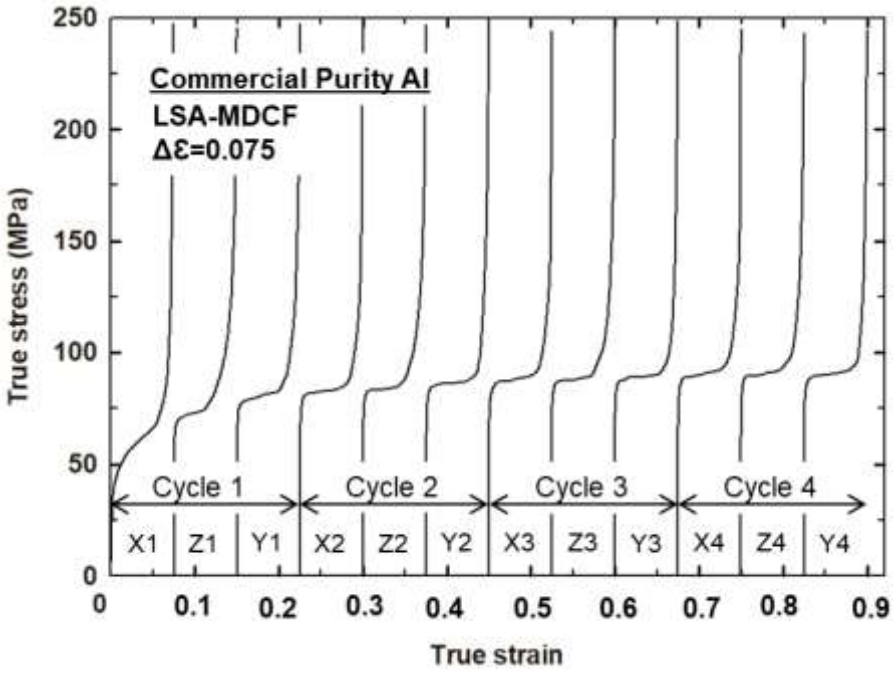

Figure 2.2 – SS curves for 4 LSA-MCDF cycles; each compression is indicated by a letter, corresponding to the compression direction, and a number, corresponding to the LSA-MDCF cycle.

A magnified inspection of the SS curves in Figure 2.2 reveals that, after the first X1 compression step, some of the SS curves exhibit a mild initial stress peak, as already observed for the LSA-MDF with re-machined specimens [13]. Figure 2.3 schematically illustrates such a curve: up to point A, a mild initial stress peak is observed, followed by a region displaying a positive work hardening rate. The curve for compression X1 obviously exhibits a pronounced initial work hardening, typical of annealed materials; in addition, some of the SS curves do not display the initial stress peak. Initial stress peaks in the SS curves are also reported in the literature for processing under plane strain confinement [20], but are much more pronounced that the present ones. It has been considered that such peaks are related to the destabilization of the dislocation structures in the specimens caused by changes in the straining direction and to "cross-test" effects [15, 30]. Curve AB includes the confining effect of the die walls; the absence of this confinement would lead to a material behavior possibly following curve AC in Figure 2.3.

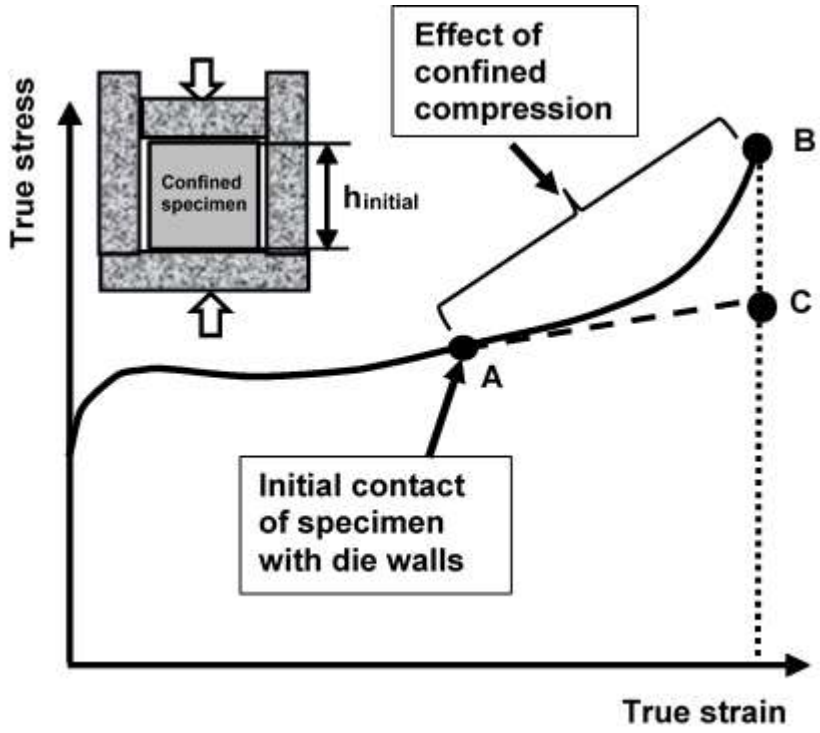

Figure 2.3 – Schematic SS curve for a compression step during LSA-MDCF

Up to the point of contact of the specimen with the lateral die walls, the SS curves in Figure 2.2 and illustrated in Figure 2.3 show close resemblance with the SS curves obtained through unconfined simple compression with re-machined specimens [13]. In the present experiments, the strain corresponding to these contact points was estimated, for every compression step, through the determination of the strain where the steadily increasing slope begins (disregarding the slope variations corresponding to eventual initial stress peaks). Figure 2.4 displays the resulting SS curves up to these strains. The expanded stress range in this figure allows a better appreciation than Figure 2.2, of the initial mild stress peaks in some SS curves.

A comparison of the curves in Figure 2.4 with those in free-compression with re-machined specimens before each compression [13] reveals that the plastic flow for both processing techniques are very similar. In addition, the elastic part of the SS curves in all LSA-MDCF compressions correspond to practically vertical lines, which is not observed in all SS curves for the re-machined specimens. The specimen shapes generated by LSA-MDCF are almost perfect and flat-faced (see the inset in Figure

2.4), because the precision machined confining die eliminates even small non-parallelism of opposing specimen faces, which occur for re-machined samples due to the inversion of the specimen position in the lathe chuck for the machining of opposing specimen faces.

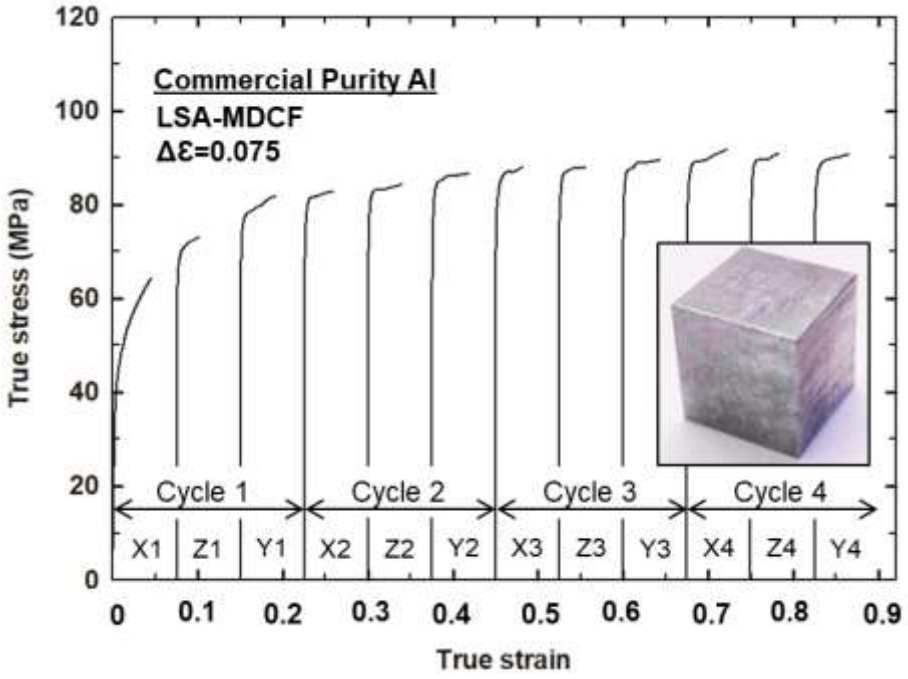

Figure 2.4 – SS curves for 4 LSA-MDCF cycles up to the strain, in each compression step, where the inflexion in the SS curve occurs.

Accordingly, it is consistently demonstrated in this investigation that LSA-MDCF is superior to LSA-MDF with and without specimen re-machining after each compression step regarding (i) the elimination of problems in the SS curves caused by the compression of irregular and non-parallel surfaces, (ii) difficulties related to the measurement of the initial dimensions of distorted specimens before each compression step and consequently in the calculation of stresses and strains (iii) time, cost and complexity associated with specimen re-machining after each compression step.

In order to compare the microstructural evolution in commercial purity Al during MDF with (MDCF) and without die confinement, Figures 2.5 and 2.6 display orientation

imaging microscopy (OIM) images and EBSD quality patterns for specimens processed through either 1 or 4 cycles of MDF, respectively. It is readily seen in Figure 2.5 that after 1 cycle of LSA-MDF the Al grain structures are somewhat distorted and exhibit similar sizes, regardless of the variation of the MDF procedure. Furthermore, a more detailed inspection of the quality patterns in Figures 2.5 (b) and (d) reveal that the EBSD analyses were unable to detect the development of well-defined sub-grains at this processing stage ($\varepsilon \approx 0.225$). This behavior is consistent with the SS curves depicted in Figure 2.4 as the material has not reached a saturation flow stress characteristic of deformation processes assisted by dynamic recovery.

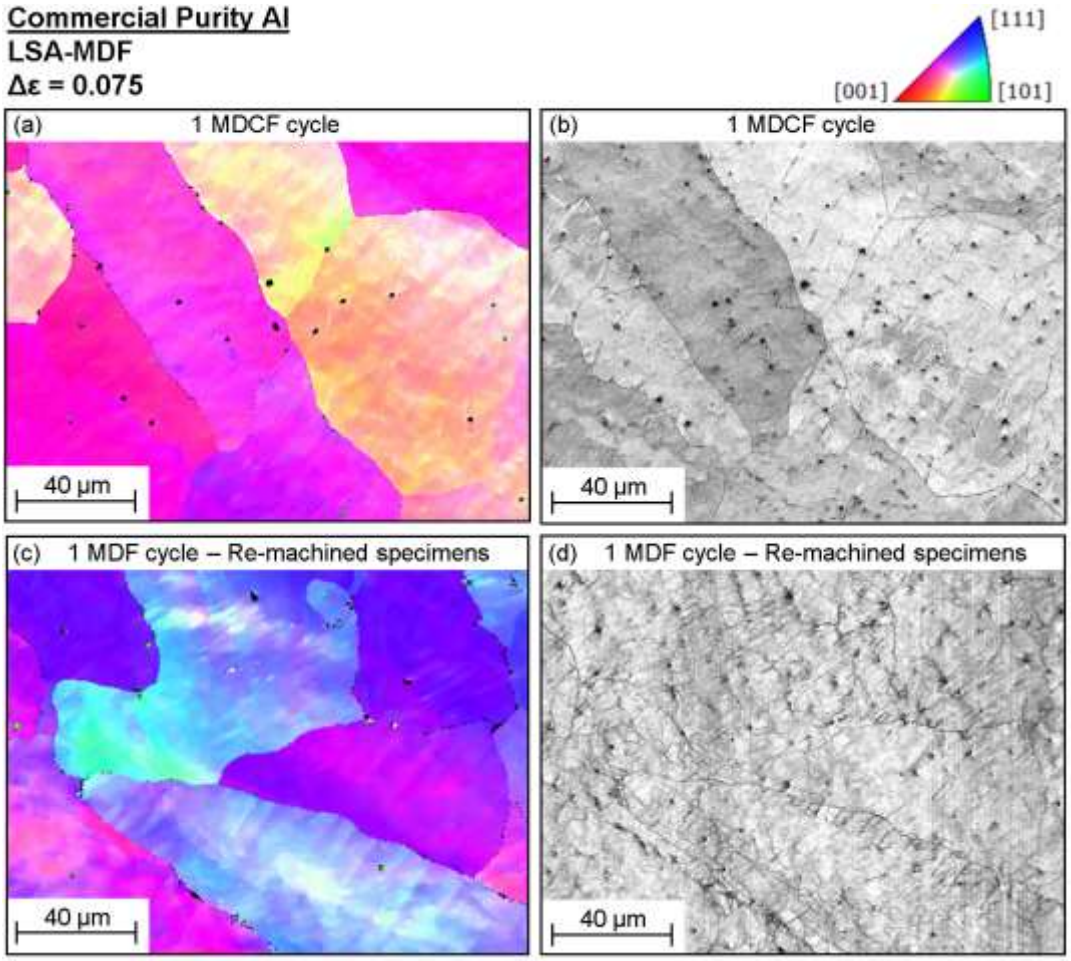

Figure 2.5 – OIM images and EBSD pattern quality maps for Al specimens processed through 1 cycle of LSA-MDF (a,b) with or (c,d) without die confinement.

Conversely, it is consistently demonstrated in Figure 2.6 that the development of homogeneously distributed sub-grains in the Al specimens deformed up to a total strain of ~0.9. The observed microstructures are typical of those generated by extensive dynamic recovery in metals with high stacking fault energy [31]. It should be noted that the grains displayed in the OIM images in Figures 2.6 (a) and (c) were colored according to the orientation triangle at the top of Figures 2.5 and 2.6. Accordingly, each color represents a different crystal orientation in relation to a plane normal to the plane of these images. It is apparent from these representative OIM images that the Al specimens exhibit similar micro-textures after processing by MDCF or MDF using free-compressions. A strong texture component develops around {110} and {100} which is typical for face centered cubic metals after compressive straining [32-33].

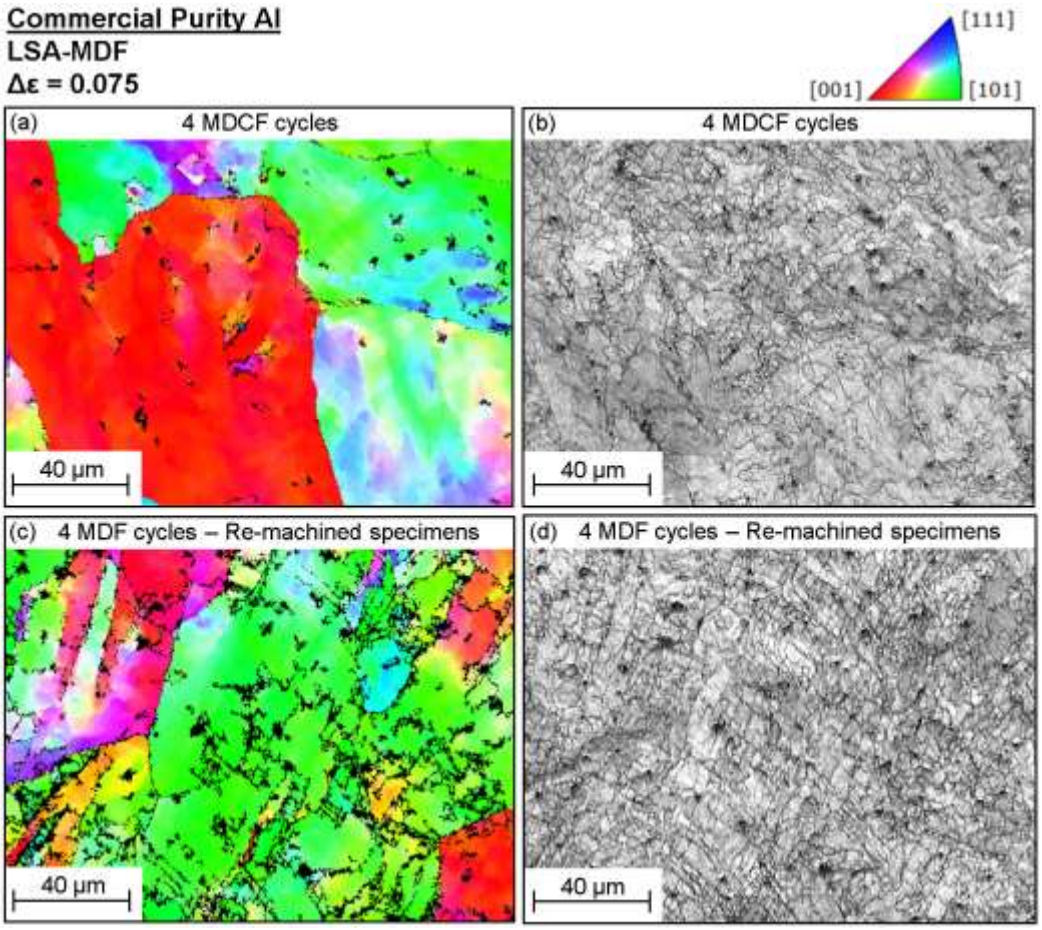

Figure 2.6 – OIM images and EBSD pattern quality maps for Al specimens processed through 4 cycles of LSA-MDF (a,b) with or (c,d) without die confinement.

The EBSD quality patterns in Figures 2.6 (b) and (d) reveal the development of nearly equiaxed sub-grain structures in commercial purity aluminum after 4 cycles of MDF with and without die confinement. The mean size of these substructural domains was estimated in these images using the linear intercept method to give average sizes of ~1.9 and 1.7 μm for the material processed through MDCF and free-compression MDF, respectively. A more thorough comparison of each OIM image and its corresponding quality pattern also shows that there remain areas in which the sub-grains are not fully developed and these regions are mostly associated with grains not displaying a strong texture component around {110}.

With the aim of better visualize the substructures formed during MDF processing, Figure 2.7 displays TEM images taken at the center of Al specimens processed by 4 cycles of LSA-MDF (a,b,c) with or (d,e,f) without die confinement. It is readily apparent from these images that the Al specimens exhibit very similar substructures after 4 MDF cycles. Most of the areas of the MDF-processed samples display well-defined subgrains having a relatively low amount of free intrinsic dislocations. Nevertheless, as evident in Figure 2.7 (d) few regions of the microstructures generated through MDF using free-compression still depict dislocation cells with diffuse walls exhibiting a high amount of free dislocations in their vicinity. Inspection of Figures 2.6 (b) and (d) and Figure 2.7 also consistently shows that both variations of MDF processing generate subgrains with comparable sizes and shapes, thus confirming the similarity of results for LSA-MDCF and for LSA-MDF with re-machined specimens.

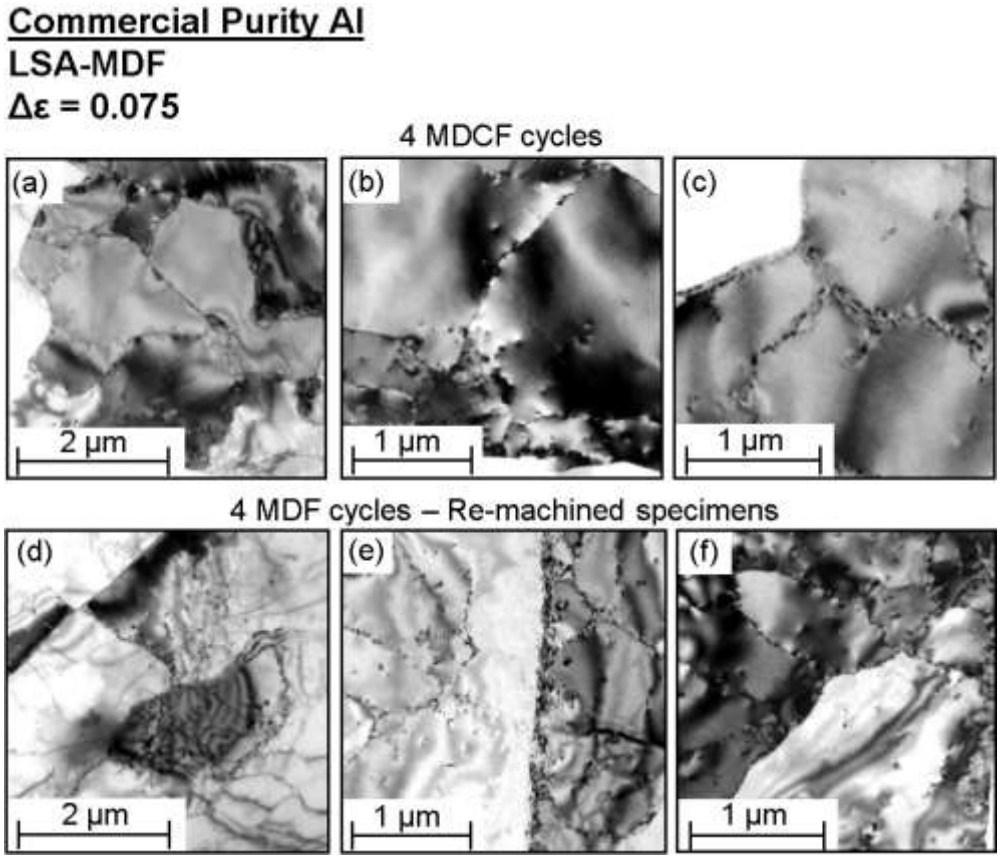

Figure 2.7 – TEM images for Al specimens processed through 4 cycles of LSA-MDF (a,b,c) with or (d,e,f) without die confinement.

2.5 CONCLUSIONS

Low Strain Amplitude Multi-Directional Confined Forging (LSA-MDCF) of aluminum, with strain amplitude $\Delta\varepsilon = 0.075$, allows the determination of adequate in-situ SS curves for each compression step, up to strains corresponding to the contact of the lateral faces of the specimens with the confining die walls.

The microstructures at the center of the specimens after 4 LSA-MDCF cycles are very similar to those for LSA-MDF with re-machined specimens. Both techniques generate refined microstructures exhibiting profuse sub-grain formation having virtually the same average size.

MDCF is practical, simple, fast, eliminates the need for specimen re-machining after each compression step, follows a strain path similar to that under simple compression, leads to an adequate determination of the in-situ stress-strain curves for each compression step, and should thus be considered as a preferential route for severe plastic deformation with MDF.

2.6 ACKNOWLEDGMENTS

Material was supplied by Novelis do Brasil. Coordenação de Aperfeiçoamento de Pessoal de Nível Superior - Brasil (CAPES) - Finance Code 001 and CNPq (National Council for Research and Technological Development) Grant 301034/2013-3 financed this research.

2.7 REFERENCES

[1] Valiev RZ, Langdon TG. Principles of equal-channel angular pressing as a processing tool for grain refinement. Progress in Materials Science. 2006; 51: 881-981.

[2] Zhilyaev AP, Langdon TG. Using high-pressure torsion for metal processing: fundamentals and applications. Progress in Materials Science. 2008; 53: 893-979.

[3] Sakai T, Belyakov A, Kaibyshev R, Miura H, Jonas JJ. Dynamic and post-dynamic recrystallization under hot, cold and severe plastic deformation conditions. Progress in Materials Science. 2014; 60: 130-207.

[4] Xu X, Zhang Q, Hu N, Huang T, Langdon TG. Using an Al–Cu binary alloy to compare processing by multi-axial compression and high-pressure torsion. Materials Science and Engineering A. 2013; 588: 280-7.

[5] Estrin Y, Vinogradov A. Extreme grain refinement by severe plastic deformation: A wealth of challenging science. Acta Materialia. 2013; 61(3) : 782-817.

[6] Quiao XG, Gao N, Morktadir Z, Kraft M, Starink MJ. Fabrication of MEMS components using ultrafine-grained aluminium alloys. Journal of Micromechanics and Microengineering. 2010; 20(4) : 1-13

[7] Xu J, Li J, Shan D, Guo B. Microstructural evolution and micro/meso-deformation behavior in Pure copper processed by equal-channel angular pressing. Material Science and Engineering A. 2016; 664: 114-25.

[8] Chan WL, Fu MW. Experimental studies of the size effect affected microscale plastic deformation in micro upsetting process. Material Science and Engineering A. 2012; 534: 374-83

[9] Kawasaki M, Langdon TG. Principles of superplasticity in ultrafine-grained materials. Journal of Materials Science. 2007; 42(5): 1782-96.

[10] Armstrong PE, Hockett JE, Sherby OD. Large strain multidirectional deformation of 1100 aluminum at 300 K. Journal of the Mechanics and Physics of Solids. 1982; 30: 37-58.

[11] Zhu QF, LI L, Ban CY, Zhao ZH, Zuo YB, Cui JZ. Structure uniformity and limits of grain refinement of high purity aluminum during multi-directional forging process at room temperature. Transactions of Nonferrous Metals Society of China. 2014; 24: 1301-6.

[12] Faria CG, Almeida NGS, Aguilar MTP, Cetlin PR. Increasing the work hardening capacity of equal channel angular pressed (ECAPed) aluminum through multi-axial compression (MAC). Materials Letters. 2016; 174: 153-6.

[13] Stemler PMA, Flausino PCA, Pereira PHR, Faria CG, Almeida NGS, Aguilar MTP, et al. Mechanical behavior and microstructures of aluminum in the Multi-Axial Compression (MAC) with and without specimen re-machining. Materials Letters. 2019; 237: 84-7.

[14] Valiev RZ, Islamgaliev RK, Alexandrov IV. Bulk nanostructured materials from severe plastic deformation. Progress in Materials Science. 2000; 45; 103-89.

[15] Li YJ, Blum W. Strain rate sensitivity of Cu after severe plastic deformation by multiple compression. Physica Status Solidi. 2005; 202: 119-21.

[16] Li YJ, Zeng XH, Blum W. On the elevated-temperature deformation behavior of polycrystalline Cu subjected to predeformation by multiple compression. Materials Science and Engineering A. 2008; 483: 547-50.

[17] Kumar SSS, Raghu T. Bulk processing of fine grained OFHC copper by cyclic channel die compression. International Journal of Materials Research. 2015; 106: 1230–9.

[18] Kundu A, Kapoor R, Tewari R, Chakravartty JK. Severe plastic deformation of copper using multiple compression in a channel die. Scripta Materialia. 2008; 58: 235-8.

[19] Berghammer R, Hu W, Hasani A, Gottstein G. Production of Ultrafine Grained AlMnFe Samples by Confined Channel Die Pressing as Compared to Equal Channel Angular Pressing. Advanced Engineering Materials. 2011; 13: 232-6.

[20] Kapoor R, Sarkar A, Yogi R, Shekwat SK, Samajdar I, Chakravartty JK. Softening of Al during multi-axial forging in a channel die. Materials Science and engineering A. 2013; 560: 404-12.

[21] Zhao S, Meng C, Mao F, Hu W. Influence of severe plastic deformation on dynamic strain aging of ultrafine grained Al–Mg alloys. Acta Materialia. 2014; 76: 54-67.

[22] Zhang S, Hu W, Berghammer R, Gottstein G. Microstructure evolution and deformation behavior of ultrafine-grained Al–Zn–Mg alloys with fine η′ precipitates. Acta Materialia. 2010; 58(60): 6695-705.

[23] Liu G, Gu G, Ni S, Liu Y, Song M. Microstructural evolution of Cu–Al alloys subjected to multi-axial compression. Materials Characterization. 2015; 103: 107-19.

[24] Mu SJ, Hu WP, Gottstein G. Investigations on Deformation Behavior and Microstructure of Ultrafine Grained Two Phase Al-Mn Alloy Fabricated by Confined Channel Die Pressing. Materials Science Forum. 2008; 584-586: 697-702.

[25] El-Danaf E, Kalidindi SR, Doherty RD, Necker C. Deformation texture transition in brass: critical role of micro-scale shear bands. Acta Materialia. 2000; 48: 2665-73.

[26] Flausino PCA, Nassif MEL, Bubani FC, Pereira PHR, Aguilar MTP, Cetlin, PR Microstructural evolution and mechanical behavior of copper processed by low strain amplitude multi-directional forging. Material Science and Engineering A. 2019; 756: 474-83.

[27] Faria CG, Almeida NGS, Bubani FC, Balzuweit K, Aguilar MTP, Cetlin, PR. Microstructural evolution in the low strain amplitude multi-axial compression (LSA-MAC) after equal channel equal pressing (ECAP) of aluminum. Materials Letters. 2018; 227: 149-53.

[28] Hussain M, Rao PN, Singh D, Jayaganthan R, Singh S. Comparative study of microstructure and mechanical properties of al 6063 alloy processed by multi axial forging at 77k and cryorolling. Procedia Engineering. 2014; 75: 129-33.

[29] Huang H, Zhang J. Microstructure and mechanical properties of AZ31 magnesium alloy processed by multi-directional forging at different temperatures. Materials Science and Engineering: A. 2016; 674: 52-8.

[30] Beyerlein IJ, Alexander DJ, Tomé CN. Plastic anisotropy in aluminum and copper pre-strained by equal channel angular extrusion. Journal of Materials Science. 2007; 42: 1733-50.

[31] Yang X, Wang D, Wu Z, YI J, Ni S, Du Y, et al. A coupled EBSD/TEM study of the microstructural evolution of multiaxial compressed pure Al and Al–Mg alloy. Materials Science and Engineering A. 2016; 658: 16-27.

[32] Hu H. Texture of Metals. Texture. 1974; 1: 233-258.

[33] Pereira PHR, Wang YC, Huang Y, Langdon TG. Influence of grain size on the flow properties of an Al-Mg-Sc alloy over seven orders of magnitude of strain rate. Materials Science and Engineering A. 2017; 685: 367-376.

3. ARTIGO II

3.1 TITLE AND ABSTRACT

Hardness, Microstructure and Strain Distributions in Commercial Purity Aluminum Processed by Multi Directional Forging (MDF)

Severe plastic deformation (SPD) of metals leads to their strengthening and grain refinement, but to low uniform elongations. Low Strain Amplitude Multi Directional Forging (LSA-MDF) is an important method for increasing this low uniform elongation. The application of workpieces of SPD-processed materials requires that their distributions of mechanical properties, microstructures and deformation be as homogeneous as possible. Analyses of these distributions after LSA-MDF have not been found in the literature, and are presented in the current investigation utilizing microhardness measurements, optical and electronic microscopy and finite element simulations. LSA-MDF causes higher strains, mcrohardeness and structural distortions in the central regions of the specimens than at their edges and corners. In addition, LSA-MDF utilizing confined compressions seems to be the preferred processing route, due to its ease and to the more homogeneous microhardness, microstructure and strain distributions in relation to other experimental procedures.

Keywords: Aluminum, Severe Plastic Deformation, Multi Directional Forging, Microstructures, Distribution of strain and microhardness.

3.2 INTRODUCTION

Severe Plastic Deformation (SPD) greatly refines grains of metals [1], leading to a remarkable strengthening and to the possibility of achieving high strain rate superplasticity [2]. Grain refinement is also important in the die filling and surface characteristics of micro-formed parts [3], which have been gaining importance due to the growing needs for miniaturization of components [4]. The most utilized SPD processing techniques are Equal-Channel Angular Pressing (ECAP) [5], High-Pressure Torsion (HPT) [6] and Multi Directional Forging (MDF)[7], also known as Multi Axial Compression[8] or Multi Axial Forging [9]. HPT produces small, thin discs; ECAP can supply bulk specimens, but involves high friction between the material and the dies

and problems such as plastic instabilities, cracks and specimen segmentation in the processing of difficult-to-work materials [2]. According to Sakai *et al.* [10], MDF has the following advantages over other SPD processing techniques: i) possible application to large (industrial) workpieces ii) allows the evaluation of the *in-situ* stress-strain characteristics of the material during processing iii) its application is simple since any testing machine or industrial press can be utilized, at various temperatures and strain rates and iv) the frequent changes in straining direction propitiates the formation of equiaxed structures. MDF is also an adequate processing route for difficult to work materials [11-13].

SPD processes have been covered in many studies in the literature and frequently focus on the evolution of the material microstructures and mechanical behavior [2,11,14]. Experimental problems in MDF derive from the specimen distortions caused by the free sequential compressions [15]. As a consequence, the measured *in-situ* stress-strain curves display inadequate results [16,17], demanding the re-machining of the specimens after each compression[18] or after a few compression steps [19]; such re-machining is time consuming, complex and costly [20]. One additional problem caused by distorted specimen faces is the measurement of the imposed strain, since the specimen displays a varying height [21]. It has also been reported that the distorted shape and surfaces of MDF specimens are a problem in ultrasonic measurements in the material [22]. MDF with confined compressions has been used in order to solve these problems [23,24], and three such approaches are found in the literature: (i) confined channel die pressing, where the material is processed under plane strain and flow confinement occurs along one of the directions orthogonal to the compression direction during all the compression, but only at the end of the compression for the other orthogonal directions [21,25-27], (ii) processing under conditions very similar to those under CCDP, but with confinement only along one of the directions orthogonal to the compression one that establishes the plane strain (hereafter denominated “open plane strain”) [8]. The lack of confinement in the other direction orthogonal to the compression direction causes distortions in the unconfined face of the workpiece [28], eventually leading to the need of its flattening through machining [23], (iii) Multi-Directional Confined Forging (MDCF), where the lateral expansion of the material caused by the

compression occurs initially in a way similar to the free compression, and then is equally confined in both directions orthogonal to the compression direction [20], leading to flat lateral faces of the specimen after each compression step. In addition, it should also be remembered that the strain path under plane strain confined processing is not the same of that in free MDF or MDCF, thus leading to differences in the microstructural and mechanical properties evolution of the material [29].

The understanding of the relationship between the microstructures and properties of materials and of the strain distribution in specimens processed through SPD has progressed appreciably in the last decade [30,31]. Heterogeneous strain distributions cause non-uniform microstructures and mechanical properties at different regions of the processed material[28], which is undesirable in the production of material to be used in any given application. The available studies on strain distributions often utilize two techniques: microhardness measurements and finite element simulations. The former has been used for the various SPD processes and their variables; an example (among many others) is the analysis of ECAP for various materials, such as pure Aluminum, 6061 Aluminum alloy and Cu-Zr alloy [32-34], covering the influence of the external die angle [35,36] and the annealing of the material after 1 ECAP pass [37]. Microhardness measurements, for example, has been used for HPT, covering studies along the disc diameters of pure Aluminum and Aluminum alloys [38-39], Zn–22% Al alloys [40,41], Mg alloys AZ31 and AZ91 [31,42], and along the thickness of disks of pure Aluminum [37,43-45]. Microhardness distribution analyses in MDF utilizing microhardness measurements have been less frequent than for ECAP and HPT, and have been performed along a line in the workpiece for open plane strain MDF [8], CCDP [24], free compressions [46] or over the full specimen cross-section in open plane strain [28], and CCDP [47,48]. The results report a higher hardness in the central regions of the workpieces than in the regions close to their borders, and that hardness in both regions tend to saturate as high levels of strain are reached. Investigations involving finite element simulations are not as common as those performed through microhardness measurements. Hao Huang and Jing Zhang [49] report, for MDF of Mg alloy AZ31 at ~300 ºC, ~350 ºC e ~400 ºC, that strain homogeneity decreases as the total imposed strain rises. Guo *et al.* [12] report an opposite result for the same material, similarly to

the report for CCDP by Magalhães *et al.* [48] for Copper, where the strain homogeneity increases as the accumulated strain rises.

SPD remarkably strengthens materials and refines their grains, but there is a drastic decrease in the uniform elongation of the material, caused by its low work hardening capacity under further deformation [30]. As a consequence, these materials do not perform well under processing where tensile deformations predominate. Recent studies covering techniques for increasing the work hardening capacity of materials previously deformed by SPD have emphasized the application of a few cycles of LSA-MDF [16] in commercial purity Aluminum. LSA-MDF has received very limited attention in the literature [13] and, as far as the authors are aware of, no results have been presented for the distribution of hardness, microstructures and strain in the processed specimens. It should be remarked that, due to the low strain amplitude in LSA-MDF, its use in order to reach the high strains typical of SPD processes would involve a very high number of compressions and thus a low productivity. The objective of the present study is the evaluation of the distributions of hardness, microstructures and strain in the LSA-MDF of commercial purity Aluminum processed under three conditions: free compressions, free compressions with specimen re-machining after each compression, and MDCF. Analyses were performed through microhardness measurements, finite element simulations and microstructural analyses employing Optical Microscopy (OM) and Electron Back Scattered Diffraction (EBSD).

3.3 EXPERIMENTAL PROCEDURE

The material was a commercially pure Aluminum (99.77wt% Al, 0.146wt% Fe, 0.060 wt% Si), received in the as-cast condition; the billet had a diameter of ≈ 150mm and was ≈ 1,500mm long. The material underwent an initial ECAP pass followed by annealing at 673K for 1h [17,20].

Three types of MDF processing were utilized in the present research, in order to compare the influence of the processing on the results: (i) free compression of the specimens, without any lateral confinement of the material flow, (ii) free compression of re-machined specimens after each compression step, in order to obtain flat surfaces to contact the compression platens in the following compression, according to a

procedure already utilized previously [17] and (iii) compression with confined dies (Multi-Directional Confined Forging, MDCF), as described elsewhere [20]. Specimens were machined out of the annealed material as cuboids with dimensions 13.00 x 12.52 x 12.06 mm along directions X, Z and Y of the specimen respectively, for both free and MDCF, and with dimensions 15.58 x 15.00 x 14.45 mm for processing with re-machining of the specimens after each compression step [17]. These larger initial dimensions were adopted in order to have specimens with approximately the same dimensions, after the complete processing of the specimens and along the three adopted MDF routes. For the case of the re-machined specimens, the successive machining of the specimen faces decreases the specimen dimensions. For the free compressions and MDCF, compressions start along the specimen axis displaying the longest edge length (X axis, measuring 13.00 mm) down to 12.06 mm, imposing a strain of $\Delta\varepsilon = 0.075$. After this first compression, the edge along the Z direction of the specimen will be 13.00 mm long, and along the Y direction 12.52 mm long. The new longest dimension, along the specimen Z axis, will then be compressed to 12.06 mm; finally, the edge along the Y axis will also be compressed from 13.00 mm to 12.06mm. After this last compression, the specimen will have been subjected to a total strain $\varepsilon = 3 \times 0.075 = 0.225$ and will have returned to its initial dimensions along the original X, Z and Y axes, corresponding to a so-called MDF "cycle". For the case of re-machined specimens, compressions also started along the longest compression and imposed a strain $\varepsilon = 0.075$; the second compression was preceded by the machining of the face to be compressed and the measurement of the initial height of the specimen along the normal to this plane, followed by a compression with $\varepsilon = 0.075$ and so on. One and four such cycles were employed leading to a total accumulated strain $\varepsilon = 0.225$ and 0.9, respectively [16,20].

Microhardness measurements and microstructural characterizations were performed on a specimen mid-plane normal to the X direction and after 1 and 4 MDF cycles, as illustrated in Figure 3.1. The sectioned specimens were mechanically ground down to a grit paper with 400 grains/cm² and then electrolytically polished at ≈ 35V for ≈ 45s with a solution of 700 ml ethylic alcohol, 120 ml of distilled water, 100 ml butyl glycol and 68ml perchloric acid, with a stainless steel cathode. Vickers microhardness

measurements were performed with a Mitutoyo model MVK-H1 tester, with a load of 2.943N applied for 15 s. Microhardness mapping involved measurements distributed on the specimen section, with a distance of 0.5 mm between the indentations both along directions Y and Z. In the case of MDCF specimens, where the specimen cuboid shape is maintained throughout the processing, the measurements reached a distance of 0.5 mm from the specimen edge, as described in Figure 3.1. Free MDF involves lateral expansion of the specimens and concave specimen surfaces, and re-machined specimens employ initially larger specimens than for free MDF and MDCF; for these cases, microhardness measurements started at the center of the specimens and the same mesh points as in MDCF. As a result, the distance of the outermost measurements from the specimen borders were larger than 0.5 mm. The results reported in the present report cover only the area of the mesh displayed in Figure 3.1.

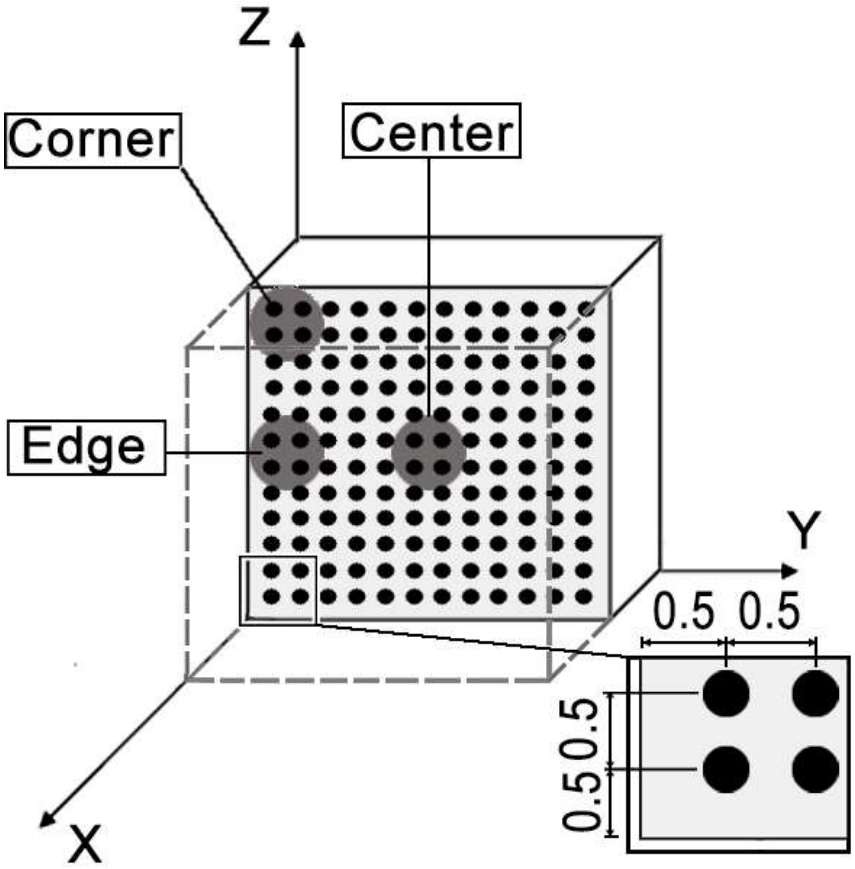

Figure 3.1. Specimen section and locations where microhardness measurements were taken and regions (center, edge and corner) where microstructural evaluations were performed.

Microstructural analyses were performed in the specimen centers, edges and corners, as indicated in Figure 3.1, for all processing conditions. Optical Microscopy (OM) utilized a Leica DM4500 P LED microscope. Electron Back Scattered Diffraction (EBSD) employed a FEI Scanning Electron Microscope (SEM) model Quanta FEG 3D and the ATEX software for the EBSD data analysis. A step size of 810 nm was used; it was verified that no relevant differences were detected in the EBSD results when lower step sizes were employed, for the present objectives. Specimen surface preparation was the same as that for microhardness measurements, but OM included an anodizing process after the mechanical and chemical polishing, using 20V for 360s and a solution of 4.5ml fluoroboric acid in 200ml distilled water and a stainless steel cathode. Images were collected using polarized light.

Computational finite element simulations of the processing were completed for the three adopted processing routes, using the commercial DEFORM 3D V11.1 software. Free compressions without re-machining of the specimen allowed the gravitational positioning of the specimens caused by the bulged lateral surfaces to be compressed, caused by the previous compression. The re-machining of the specimen was performed numerically through the minimal elimination of the bulged volume in the face to be compressed, till a flat face was obtained, normal to the respective cuboid axis. MDCF and free compression simulations involved rigid dies. The constitutive behavior of the material was taken as the envelope of the individual stress-strain curves for every compression step with confining dies, already reported by the present authors [20]. The material was considered as isotropic and insensitive to strain rate variations. The coefficient of friction between the material and the compression dies was taken as 0.4, which led to a very similar external shapes of the specimens in the simulation and in the experiments with specimen re-machining. The element density was 10.11 elements/mm^3, the punch speed was 0.05 mm/s and the punch displacement per step was 0.047mm/step.

It is recognized that the simulation results for the specimen shape, strain and stress distributions are approximate due to the following points: the constitutive behavior is described by a monotonically increasing flow stress corresponding to the envelope of the individual stress stress-strain curves for each MDCF compression. These display

decreased yield strengths in relation to the corresponding flow stress in the envelope curve, as well as initial mild stress peaks [20,50], associated with the strain path changes as the specimen is rotated. These phenomena cannot be accounted for in the current state of finite element simulations. In addition, material anisotropy is always present due to its crystallographic texture and was not considered in the simulations. As a consequence, the distortions in the specimens can be underestimated and thus their influence on the obtained strain distributions can be below the experimental ones.

3.4 RESULTS

3.4.1 Specimen shape and microhardness distributions

Figure 3.2 exhibits the shapes of the mid-section of the processed specimens (see Figure 3.1), as well as the microhardness distributions on these sections, for the three MDF techniques in the present investigation and for 1 and 4 MDF cycles. Free MDF without specimen re-machining leads to increasingly rhomboidal specimens, starting from the 1st MDF cycle (Figure 3.2a) and more distorted by the successive MDF cycles, as evidenced in Figure 3.2b (after the 4th MDF cycle). MDF with free compressions also led to higher hardness values along the smaller rhomboid diagonal, again starting from the 1st MDF cycle (Figure 3.2a) and enhanced after the 4th MDF cycle (Figure 3.2b).

The results for processing with re-machined specimens and with confined compressions (Figure 3.2c – 3.2f) consistently reveal that the problems reported above for free compressions were eliminated. The dimensions of specimens re-machined after each compression are somewhat different from those for free compressions and for MDCF, since machining obviously changes the specimen dimensions. In the present experiments, the anisotropic lateral expansion of the specimens caused more material removal by machining normal to the Y direction than normal to the X and Z directions, in order to flatten the specimen face to be compressed and thus to a narrower specimen along the Y direction. This is connected to the crystallographic textures developed by the initial ECAP + annealing treatment and by the successive MDF compressions. For 1 MDF cycle (Figures 3.2c and 3.2e) the central regions of the specimens are harder than those closer to the specimen edges, as already indicated

in the literature [28]. The MDCF specimen has a lower hardness in the central region than the re-machined specimens, but a more uniform microhardness distribution. This tendency is eliminated after the 4th MDF cycle, but processing with re-machined specimens leads to a microhardness distribution where the specimen diagonals display higher hardness than the rest of the specimen, and an "X" shaped high hardness region can be observed. This situation was not detected for MDCF processing (Figure 3.2e and 2f); in addition, 4 MDCF cycles lead to a larger harder central region than the other two procedures.

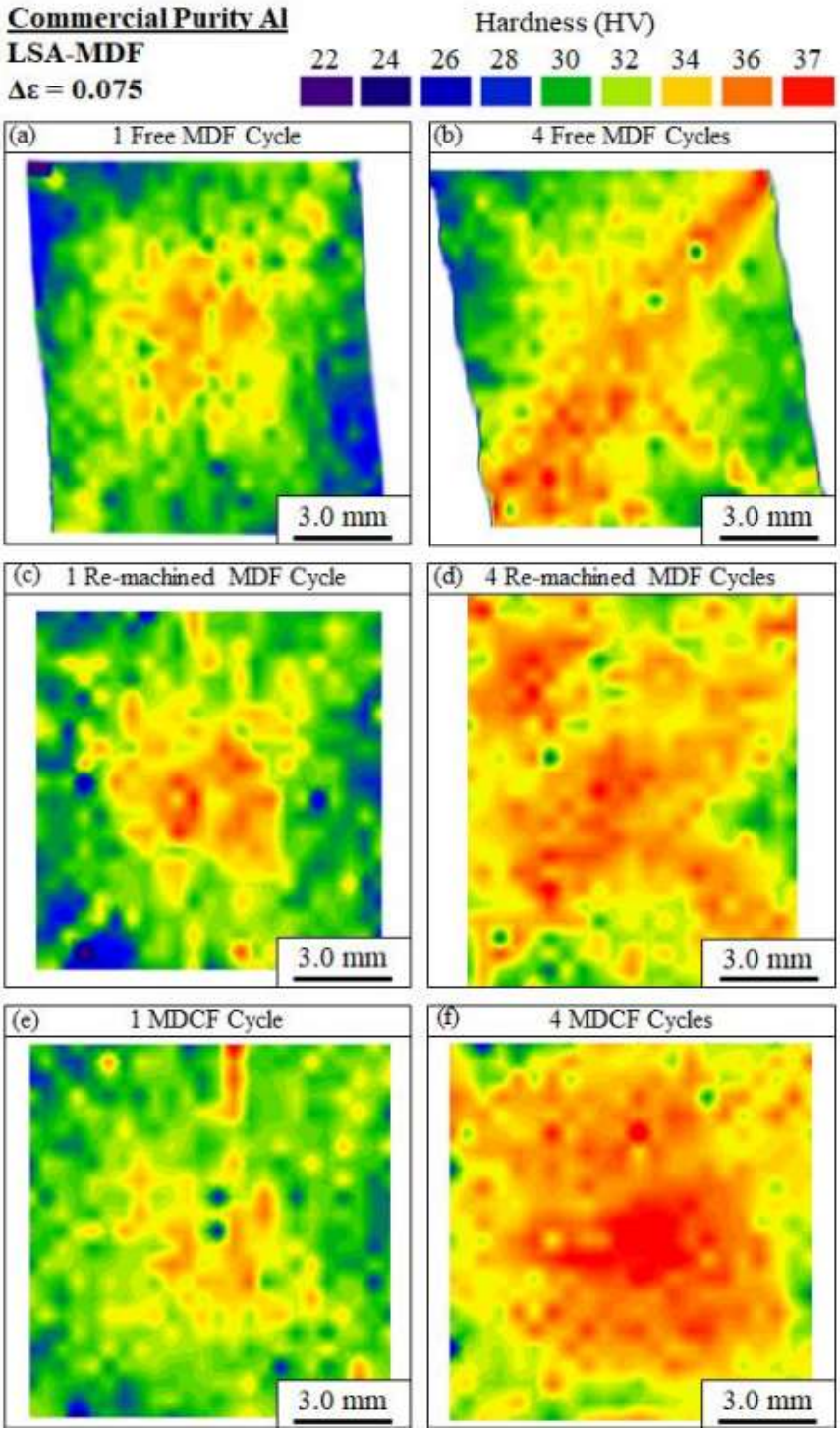

Figure 3.2. HV microhardness distributions for specimens processed for 1 and 4 MDF cycles respectively for (a, b) free MDF, (c, d) free MDF and re-machined specimens, and (e, f) MDCF.

3.4.2 Microstrutures

3.4.2.1 Optical microscopy (OM)

Figure 3.3 displays the OM (Optical Microscopy) images of the central regions of the specimens (see Figure 3.1) processed for 1 and 4 cycles of free MDF, free MDF with re-machined specimens and MDCF.

For the central region and 1 MDF cycle Figure 3.3a indicates that little deformation seems to have occurred for free MDF, since the grains are basically undistorted and exhibit practically no deformation bands. Re-machined specimens (Figure 3.3c) show some distortions of the grains and deformation bands, that would be caused by a higher deformation than in free MDF (Figure 3.3a). MDCF (Figure 3.3e) led to grains with somewhat more distortions and deformation bands than in the re-machined specimens. The images for the central region and 4 MDF cycles (Figures 3.3b, 3.3d and 3.3f) also suggest a similar increase in the deformation as the different processing routes are adopted, involving more grain distortions and deformation bands.

The above results for the central region of the specimens are similar to those observed in the specimen edges and corners (see Figure 3.1) especially after 1 MDF cycle. The qualitative situation after 4 MDCF cycles is also similar to that in Figure 3.3, but the level of grain distortions and intensity of shear banding in the edge and corner regions is lower than in the central region. These differences, however, are not very appreciable.

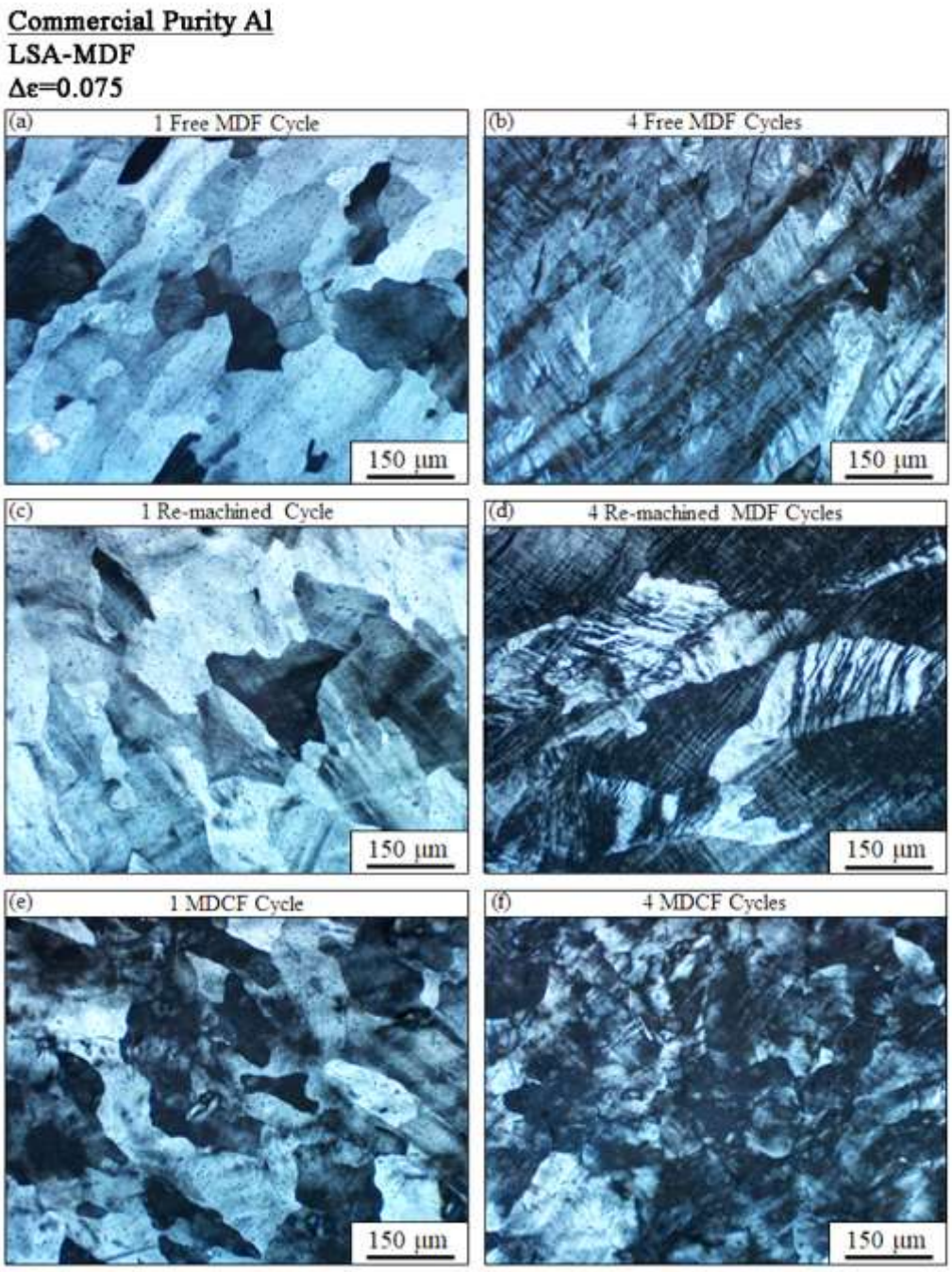

Figure 3.3. OM images of the specimen microstructures at the central regions after 1 and 4 MDF cycles respectively for (a, b) free MDF, (c, d) free MDF and re-machined specimens, and (e, f) MDCF.

3.4.2.2 Electron Microscopy

An electron microscopy analysis was performed in the annealed material and at the central, edge and corner regions of a specimen processed after 4 MDCF cycles; these results can be extended to the other two processing routes, as indicated by the microhardness and OM studies. Figure 3.4a corresponds to the annealed material, Figure 3.4b to the central specimen region, Figure 3.4c to the edge region and Figure 3.4d to the corner region. The black lines in the OIM maps correspond to grain boundaries with misorientation angles above 5º and allow their easier visualization. The color hues observed in the deformed materials (Figures 3.4b, 3.4c, 3.4d), correspond to small differences in the spatial orientation of the various regions, associated with the formation of substructures in the material inside the original grains, which are more equiaxed in the central region (Figure 3.4b) and more elongated in the edge and corner areas (Figures 3.4c and 3.4d). Some of these regions with color hues are surrounded by black lines, indicating a disorientation above 5º; in addition, some grains without internal color hues are also surrounded by black lines, suggesting the presence of a single grain orientation.

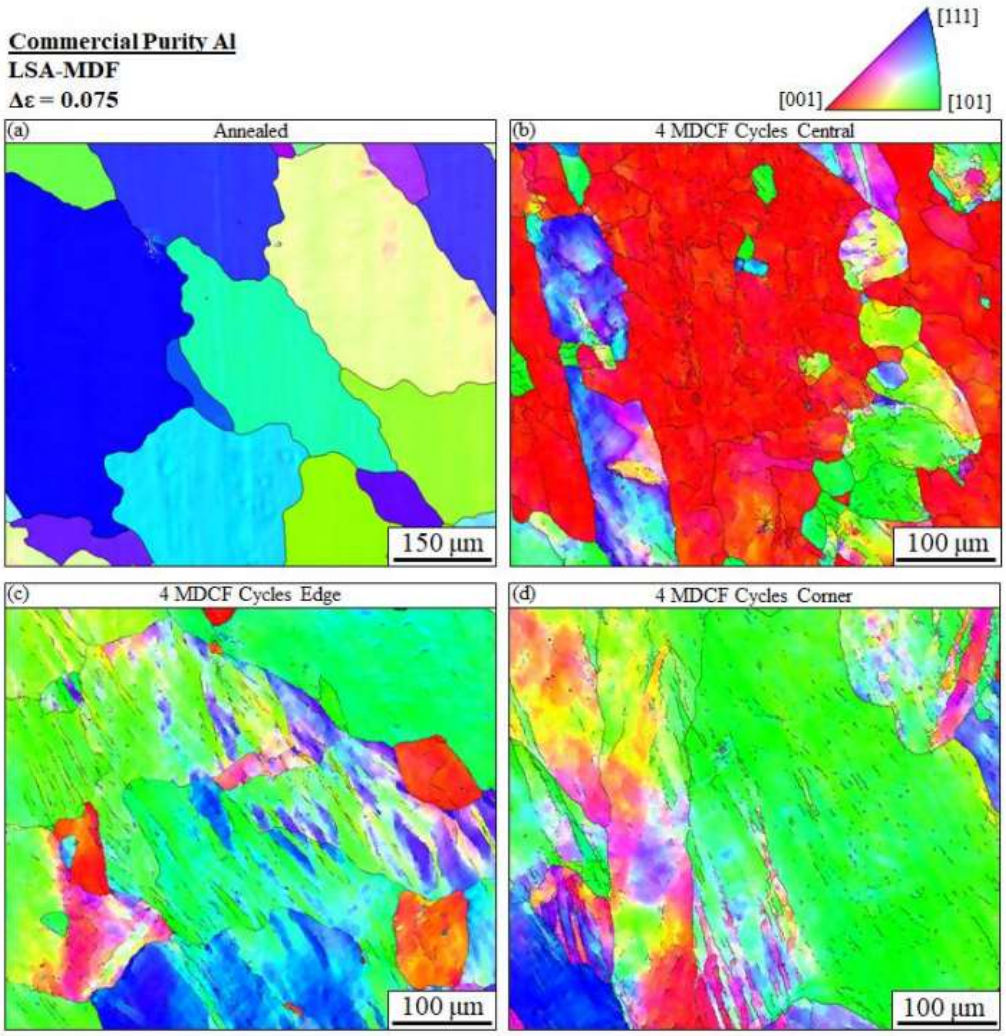

Figure 3.4. Orientation Image Mapping (OIM) of the (a) annealed material and after 4 MDCF cycles at the, (b) central, (c) edge and, and (d) corner specimen regions.

3.4.2.3 Numerical simulations

Figure 3.5 shows the results of the numerical simulations predictions for the distribution of strain and shape in the specimen mid-planes for 1 and 4 MDF cycles and for free MDF, free MDF with re-machined specimens and MDCF. The dimensions of the re-machined specimen after 1 MDF cycle are obviously higher than of the other specimens, since it will be successively machined till reaching approximately the same dimensions of the other specimens after 4 MDF cycles.

For the case of free compressions, the experimental distortions in the shape of the specimens displayed in Figures 3.2a and 3.2b were not replicated in the simulation results, probably as consequence of the lack of crystallographic texture effects in the simulations. In addition, no “X” shaped deformation pattern (see Figure 3.2d) was exhibited in any simulation. A higher strain was observed in the central regions of all specimens, in accordance with the previous findings based on microhardness measurements and microstructural analyses. The simulations also indicate that the central, more deformed region of the specimens is somewhat larger for the re-machined specimens than for the free compressions and MDCF; this is a consequence of the elimination of the outermost, less deformed regions of the specimens, due to their machining. The maximum strain in the central region of the specimens after 4 MDF cycle is about 1.4, higher than the applied external strain (0.9) and after 1 MDF cycles is about 0.26, again higher than the external strain (0.225).

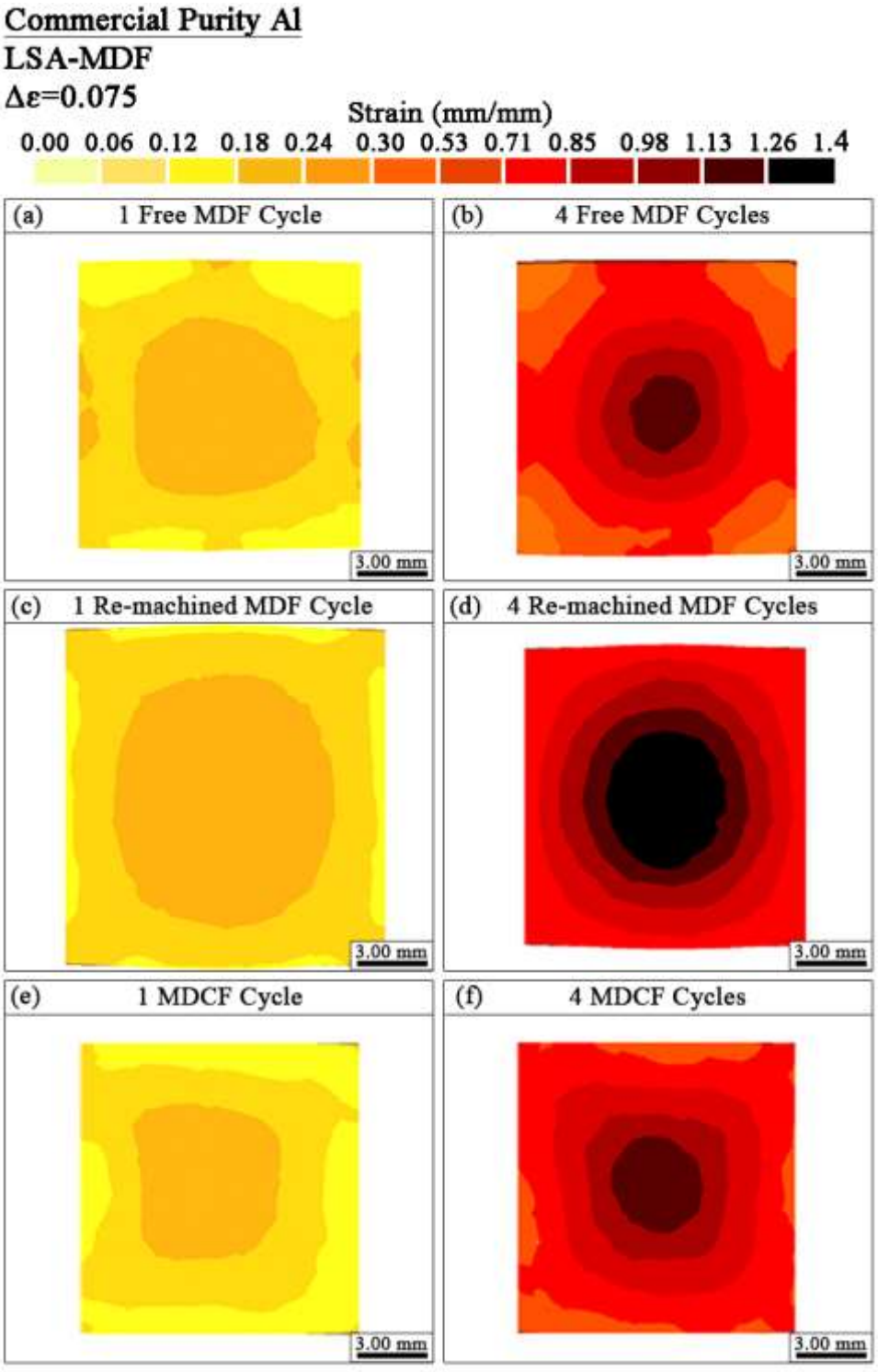

Figure 3.5. Numerical simulations prediction for the distribution of strain in the specimen mid-planes for 1 and 4 MDF cycles respectively for (a, b) free MDF, (c, d) free MDF and re-machined specimens, and (e, f) MDCF.

3.5 DISCUSSION

3.5.1 Specimen shape and microhardness distributions

The results displayed in Figures 3.2a and b indicate that free MDF leads to specimen distortions and to a heterogeneous strain distribution with higher hardness along the smaller diagonal of the distorted rhomboid. The literature also reports that free MDF is conducive to specimen distortions; Zhu *et al.*[15] show a specimen cross-section exhibiting even a concave lateral shape. Armstrong *et al.*[19] state that re-machining of specimens was necessary after a few MDF cycles in order to eliminate the specimen distortions, but does not show any example of the distortions. Free MDF of Aluminum seems thus inconvenient as a SPD processing technique, from the point of view of specimen distortions and microhardness heterogeneities.

The average hardness values for the situations described in Figure 3.2 are 30.7, 31.1 and 31.2 HV after 1 MDF cycle and 32.2, 33.5 and 33.7 HV after 4 MDF cycles for free MDF, free MDF with re-machined specimens and MDCF, respectively. The hardness of Aluminum 1070 after rotary swaging up to a deformation of 1, which is above the present strain of 0.9 for 4 MDF cycles, has been reported as 35.5 HV; in addition, the initial hardness of this material is practically identical to that in the present study [51]. These results are consistent with the present ones.

The results displayed in Figure 3.2c - f show that MDF with re-machined specimens and MDCF lead to higher hardness in the central regions of the specimens than at their borders. In addition, 4 cycles of MDF with re-machined specimens led to higher hardness along the two specimen diagonals displaying a “X” shaped harder region; similar results have already been reported in the literature for the free MDF of Aluminum [15] and for the MDF of Titanium processed in a channel die under open plane strain[28].

Microhardness profiles along the Y direction of the specimens at their Z direction mid-height were extracted from the microhardness maps data for 1 or 4 MDF cycles and the three processing routes. For a given distance from the center of the specimen, the 4 vertical microhardness measurements vertically around the centerline, spaced by 0.5

mm (see Figure 3.1), were considered for their averages and dispersion bars, similarly to the procedure adopted in the literature [33]. The results are displayed in Figures 3.6a, 3.6b and 3.6c, for free MDF, MDF with re-machined specimens and for MDCF, respectively. The horizontal line in these figures corresponds to the average hardness in the annealed specimen. The results in Figure 3.6 confirm that the central part of the specimens is harder than the regions closer to their borders. No results were found in the literature for the LSA-MAC of Aluminum up to the total deformations reported in the present investigations. On the other hand, the average hardness in the central and border regions for the Al-4%Cu alloy, after open plane strain MDF with a strain amplitude of 0.47 and after 15 compressions (total average deformation 7.05) also show that the hardness in the central region was also higher than in the border of the specimen [8].

The measurement dispersions, represented in Figure 3.6 by the error bars, are often substantially higher for processing with 1 MDF cycle than for 4 cycles. This is associated with the shape of the stress-strain curve of the material, which is typical for FCC metals with high stacking fault energy, where lower strains are linked to higher work hardening rates than higher strains. The theoretical average strain in the specimens after 1 MDF cycle is 0.225 and after 4 MDF cycles 0.9. Hardness is directly linked to the material flow stress [26]; as a consequence, at lower average strains, any local strain heterogeneities will lead to larger hardness variations than for higher average strains, as often indicated in the dispersion bars in Figure 3.6. A similar situation is reported in the literature, for microhardness measurements in Al 99.99% processed by 1 and 4 ECAP passes [33].

The comparison of Figures 3.6a and 6b indicates that free MDF with re-machined specimens (Figure 3.6b) led to somewhat higher hardness at the specimen borders than without such re-machining (Figure 3.6a). Re-machining eliminates the specimen lateral bulges caused by their compression, which are regions less deformed than the central specimen regions [15]. The specimens where no re-machining was performed thus contain lateral regions less deformed and thus softer than those in the re-machined specimens.

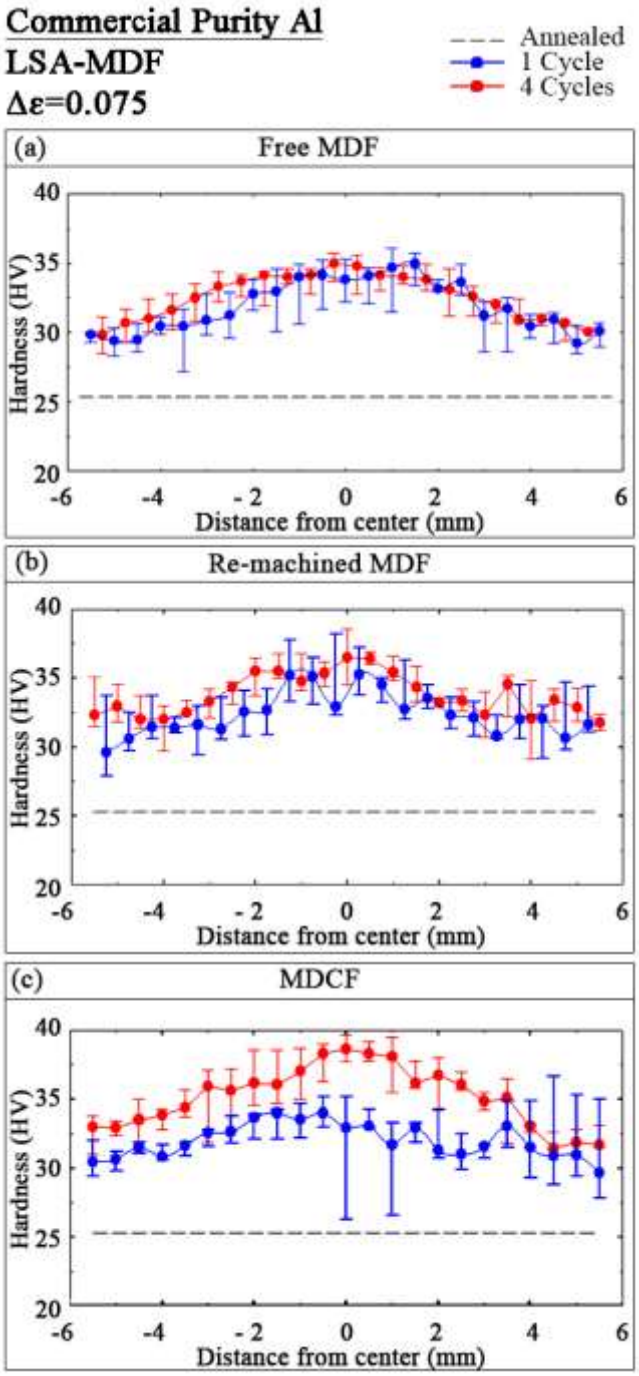

Figure 3.6. Microhardness measurements along the width of the mid-section of the processed specimens and at its mid-height, for 1 or 4 MDF cycles with (a) free MDF, (b) free MDF with re-machined specimens, and (c) MDCF (Multi Directional Confined Forging).

MDCF does not lead to lateral bulges in the specimen, due to the confinement with the die walls; in contrast to free MDF and to MDF with re-machined specimen, some additional straining and work hardening should thus occur in the lateral faces of the specimens. When the specimens are rotated, these harder regions cause more deformation in the central specimen regions than in the other two processing routes and, as a consequence, to a greater difference in the hardness curves for 1 and 4 MDF cycles, as shown in Figure 3.6c, in comparison with similar curves in Figures 3.6a and 6b, where the difference in strains caused by 1 or 4 MDF cycle seems to have not caused any appreciable hardening. Such lack of hardening is similar to that for 1 and 4 ECAP passes (involving a much higher applied strains) in high purity Aluminum[33]. These authors also report that, after 1 ECAP pass (average deformation of ≈ 1) the hardness in the specimen varies from 30 to 45 HV, which is a higher range of values than that observed in the present results (from about 26 to 34 HV, for free compressions). For the average strain levels in the present investigations, HPT leads to much higher microhardness heterogeneities than any of the present MDF procedures [39].

From the points of view of specimen distortions, microhardness distributions and ease of processing, MDCF seems to be the preferable route for LSA-MDF processing.

3.5.2 Microstructures

The optical and electron microscopy results displayed in Figures 3.3 and, 3.4, respectively, where microstructural features in the center of the specimens are more refined than at their edges and corners, are in accordance with reports in the literature, such as those of Zhu *et* al.[15] for the free MDF of high purity Aluminum. In addition, these microstructural features are in agreement with the results based on the hardness distributions (Figure 3.2) and profiles (Figure 3.6), where hardness is higher in the central parts of the specimens than in their borders.

The OIM results (Figure 3.6), indicate a relatively strong preferential orientation of the grains around the <110> and <100> directions and is typical of FCC materials subjected to compression [52-53].

Figure 3.7 displays the grain boundary characteristics at the central, edge and corner regions of a specimen processed after 4 MDCF cycles. Figures 3.7a and 3.7b refer to the central specimen region, Figures 3.7c and 3.7d to the edge and Figures 3.7e and 3.7f to the corner regions. The color lines in Figures 3.7a, 3.7c and 3.7e correspond to ranges of grain disorientations; red lines represent grain boundaries misorientation angles in the range of 2º to 5º, the green lines to the range 5º to 15º and the dark blue lines to angles above 15º. The first two groups are usually called Low-Angle Grain Boundaries (LAGBs) and the third group High-Angle Grain Boundaries (HAGBs). Figures 3.7a, 3.7c and 3.7e indicate the presence of dislocation cells/subgrains in the material in all three examined specimen regions, confirming the formation of substructures suggested by the color hues in the OIM images in Figure 3.6. These substructures are basically equiaxed in the central region (Figure 3.7a) and elongated in the edge and corner regions (Figures 3.7d and 3.7f). It is generally recognized that dislocation substructures in FCC metals with a high stacking fault energy (SFE) initially form in an elongated/lamellar aspect, and then, as strain is raised, become equiaxed[54]. This is in agreement with previous microhardness and OM results, which indicate the occurrence of higher deformations in the central region of the specimen than at its edges and corners. Figures 3.7b, 3.7d and 3.7f display the grain disorientation histograms for the three regions of the specimen. These distributions are similar and involve a low fraction of HAGBs; there is a small tendency for a higher fraction of HAGBs in the central region (0.038), in comparison with the corner (0.031) and edge (0.022) regions. This is probably connected to the increasing strain as one considers the edge, corner and central regions of the specimen, causing an increasing refinement of the structure. On the other hand, the situation should be viewed cautiously, since the differences in the measured values of HAGB fractions are low.

There was a pronounced grain refinement after the 4 MDF cycles for all processing conditions. The initial grain size of the annealed material was ~170 μm and the final grain size, considering only HAGBs (High Angle Grain Boundaries, with disorientation angles $\theta > 15^{o}$) in the central region of the specimens was 30 μm as measured through the OIM images.

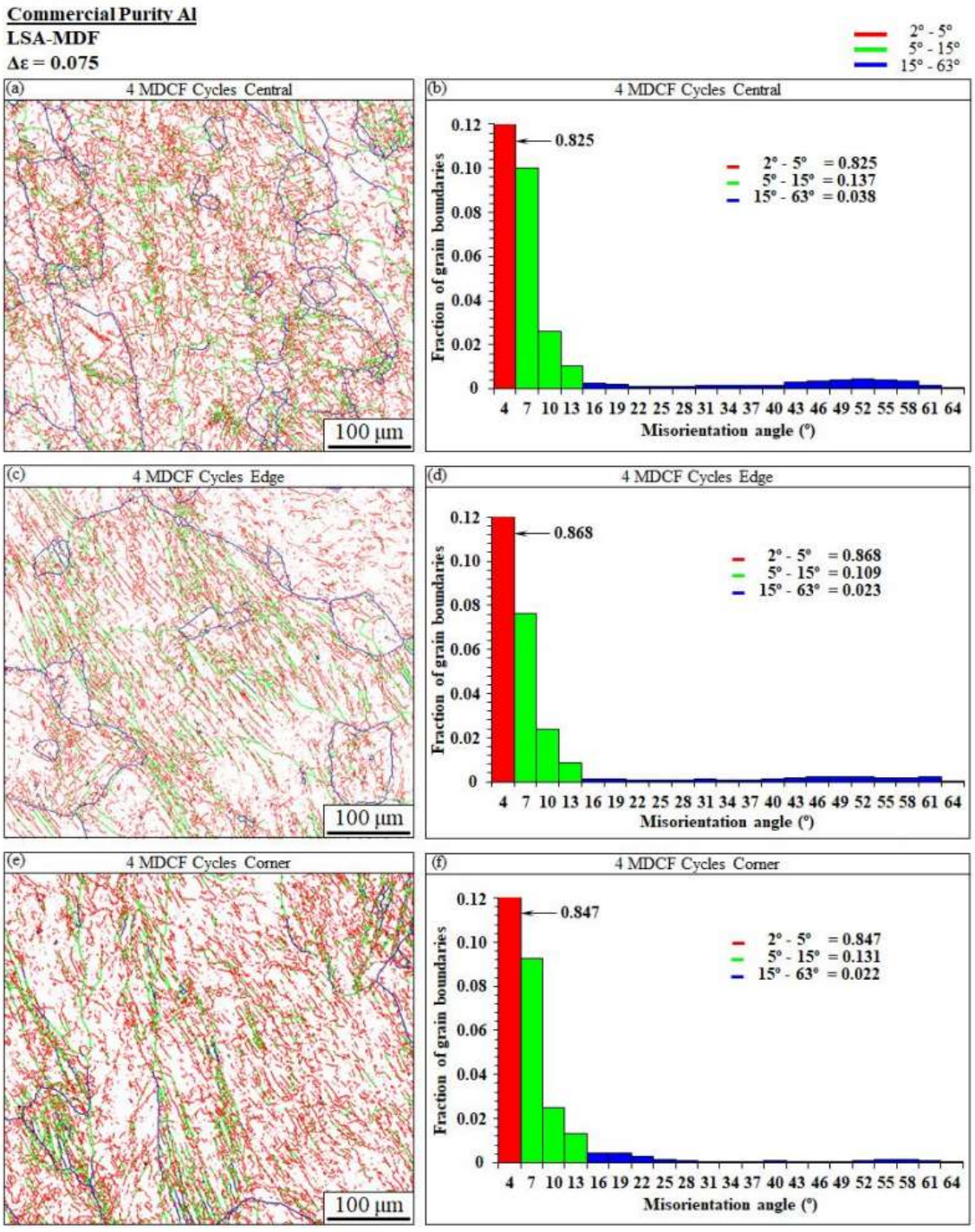

Figure 3.7. Grain boundary characteristics and distribution of grain disorientations of the material after 4 MDCF cycles, respectively (a, b) central specimen region, (c, d) edge specimen region, and (e, f) corner specimen region.

3.5.3 Simulations

The simulation results displayed in Figure 3.5 are in accordance with previous indications for the observed strain distribution, based on microhardness measurements and microstructural analyses. A higher strain is indicated for the central region of the specimen than at its edges and corners For free compressions, however, the simulations did not predict specimen distortions similar to those experimentally found, for the reasons already discussed.

The most homogeneous deformation distributions after 4 MDF cycles was obtained with specimens re-machined after each compression step. This is a consequence of the repeated removal of the outermost, less deformed regions of the specimen by machining. As already discussed, this procedure is time consuming, expensive and complex. A comparison of the strain distribution after 4 MDF cycles under free compression (Figure 3.5b) and with MDCF (Figure 3.5f), where specimen distortions were neglected for the free compression, indicates that MDCF leads to a somewhat higher uniformity of strain distribution than free compressions.

3.6 CONCLUSIONS

The present paper focuses on the analysis of the distributions of microhardness, microstructures and effective strain associated with Low Strain Amplitude MDF (LSA-MDF), after 1 and 4 LSA-MDF cycles. The results indicate that:

1. MDF under free compressions led to specimen distortions and to heterogeneous microhardness distributions. The specimens developed rhomboid sections and microhardness was higher along the shorter rhomboid diagonal than along the longer one. MDF with re-machined specimens and MDCF (Multi directional Confined Compressions) eliminated these problems;
2. Microhardness measurements, microstructure analysis and numerical simulations of specimens after LSA-MDF with re-machined specimens and with MDCF indicate that these processing techniques lead to a higher strain in the central region of the specimens than in the regions closer to the specimen faces;

3. When re-machined specimens are utilized, the outermost regions of the specimen, which display lower deformations than the central regions, are successively removed by machining; as a consequence, the microhardness and strain distributions in re-machined specimens is somewhat more homogeneous than under MDCF. Specimen re-machining is complex, time-consuming and costly;
4. The distribution of microstructures for all the LSA-MDF processing routes was similar; the central area of MDCF specimens displayed more equiaxed and refined grain structures than the corner and edge regions;
5. From the point of view of deformation through LSA-MDF, MDCF seems to be the preferred route, due to its simplicity, low cost ease and its microhardness, microstructure and strain distributions, in relation to the other procedures (free compressions and compressions with re-machined specimens).

3.7 ACKNOWLEDGEMENTS

Material was supplied by Novelis do Brasil. Coordenação de Aperfeiçoamento de Pessoal de Nível Superior - Brasil (CAPES) - Finance Code 001 and CNPq (National Council for Research and Technological Development) Grant 301034/2013-3 financed this research.

3.8 REFERENCES

[1] Langdon, TG. The principles of grain refinement in equal-channel angular pressing. Mater. Sci. Eng. A. 2007;462:3-11.

[2] Langdon, Terence G. Twenty-five years of ultrafine-grained materials: Achieving exceptional properties through grain refinement. Acta Mater. 2013; 61:7035-7059.

[3] Xu J, Shi L, Wang C, Shan D, Guo B. Micro hot embossing of micro-array channels in ultrafine-grained pure aluminum using a silicon die. J. Mater. Process. Technol. 2015;225:375-384.

[4] Fu MW, Chan WL. A review on the state-of-the-art microforming technologies. Int. J. Adv. Manuf. Tech. 2013;67:2411-2437.

[5] Valiev RZ, Langdon TG. Principles of equal-channel angular pressing as a processing tool for grain refinement. Prog. Mater. Sci. 2006;51:881-981.
[6] Zhilyaev AP, Langdon TG. Using high-pressure torsion for metal processing: Fundamentals and applications. Prog. Mater. Sci. 2008;53:893-979.
[7] Sakai T, Belyakov A, Kaibyshev R, Miura H, Jonas JJ. Dynamic and post-dynamic recrystallization under hot, cold and severe plastic deformation conditions. Prog. Mater. Sci. 2014;60:130-207.
[8] Xu X, Zhang Q, Hu N, Huang Y, Langdon TG. Using an Al–Cu binary alloy to compare processing by multi-axial compression and high-pressure torsion. Mater. Sci. Eng. A. 2013;588:280-287.
[9] Estrin Y, Vinogradov A. Extreme grain refinement by severe plastic deformation: A wealth of challenging science. Acta Mater. 2013;61:782-817.
[10] Sakai T, Miura H, Yang X. Ultrafine grain formation in face centered cubic metals during severe plastic deformation. Mater. Sci. Eng. A. 2009;499:2–6.
[11] Valiev RZ, Islamgaliev RK, Alexandrov IV. Bulk nanostructured materials from severe plastic deformation. Prog. Mater. Sci. 2000;45:103-189.
[12] Guo W, Wang Q, Ye B, Zhou H. Microstructure and mechanical properties of AZ31 magnesium alloy processed by cyclic closed-die forging. J. Alloys Compd. 2013;558:164-171.
[13] Flausino PCA, Nassif MEL, Bubani FC, Pereira PHR, Aguilar MTP, Cetlin PR. Microstructural evolution and mechanical behavior of copper processed by low strain amplitude multi-directional forging Mater. Sci. Eng. A. 2019;756:474-483.
[14] Alhajeri SN, Gao N, Langdon TG. Hardness homogeneity on longitudinal and transverse sections of an aluminum alloy processed by ECAP. Mater. Sci. Eng. A. 2011;528:3833-3840.
[15] Zhu QF, Lei LI, Ban CY, Zhao ZH, Zuo YB, Cui JZ. Structure uniformity and limits of grain refinement of high purity aluminum during multi-directional forging process at room temperature. T. Nonferr. Metal Soc. 2014;24:1301-1306.
[16] de Faria CG, Almeida NGS, Aguilar MTP, Cetlin PR. Increasing the work hardening capacity of equal channel angular pressed (ECAPed) aluminum through multi-axial compression (MAC). Mater. Lett. 2016;174:153-156.

[17] Stemler PM, Flausino PC, Pereira PH, de Faria CG, Almeida NG, Aguilar MTP, Cetlin PR. Mechanical behavior and microstructures of aluminum in the Multi-Axial Compression (MAC) with and without specimen re-machining. Mater. Lett. 2019;237:84-87.

[18] Li YJ, Zeng XH, Blum W. On the elevated-temperature deformation behavior of polycrystalline Cu subjected to predeformation by multiple compression. Mater. Sci. Eng. A. 2008;483:547-550.

[19] Armstrong PE, Hockett, JE Sherby OD. Large strain multidirectional deformation of 1100 aluminum at 300 K. J. Mech. Phys. Solids. 1982;30:37-58.

[20] Almeida NGS, Pereira PHR, de Faria CG, Aguilar MTP, Cetlin PR. Mechanical behavior and microstructures of aluminum processed by low strain amplitude multi-directional confined forging. J. Mater. Res. Technol. 2020;9:3190-3197.

[21] Kapoor R, Sarkar A, Yogi R, Shekhawat SK, Samajdar I, Chakravartty JK. Softening of Al during multi-axial forging in a channel die. Mater. Sci. Eng. A. 2013;560:404-412.

[22] Yaghoubi F, Moghanaki SK, Kazeminezhad M. Sound velocity in severely deformed aluminum alloys: AA1100 and AA2024. Appl. Phys. A-Mater. 2020;126:1-10.

[23] Kundu A, Kapoor R, Tewari R, Chakravartty JK. Severe plastic deformation of copper using multiple compression in a channel die. Scr. Mater. 2008;58:235-238.

[24] Ghanbari BF, Arabi H, Abbasi SM, Boutorabi SMA. Manufacturing of nanostructured Ti-6Al-4V alloy via closed-die isothermal multi-axial-temperature forging: microstructure and mechanical properties. Int. J. Adv. Manuf. Tech. 2016;87:755-763.

[25] Mu SJ, Hu WP, Gottstein G. Investigations on deformation behavior and microstructure of ultrafine grained two phase Al-Mn alloy fabricated by confined channel die pressing. Mater. Sci. Forum. 2008;584:697-702.

[26] Zhang S, Hu W, Berghammer R, Gottstein G. Microstructure evolution and deformation behavior of ultrafine-grained Al–Zn–Mg alloys with fine η′ precipitates. Acta Mater. 2010;58:6695-6705.

[27] Parimi AK, Robi PS, Dwivedy SK. Severe plastic deformation of copper and Al–Cu alloy using multiple channel-die compression. Mater. Des. 2011;32:1948-1956.

[28] Kumar SS, Priyasudha K, Rao MS, Raghu T. Deformation homogeneity, mechanical behaviour and strain hardening characteristics of titanium severe plastically deformed by cyclic channel die compression method. Mater. Des. 2016;101:117-129.
[29] El-Danaf E, Kalidindi SR, Doherty RD, Necker C. Deformation texture transition in brass: critical role of micro-scale shear bands. Acta Mater. 2000;48:2665-2673.
[30] Sabirov I, Murashkin MY, Valiev RZ. Nanostructured Aluminum alloys produced by severe plastic deformation: New horizons in development. Mater. Sci. Eng. A. 2013;560:1-24.
[31] Al-Zubaydi A, Figueiredo RB, Huang Y, Langdon TG. Structural and hardness inhomogeneities in Mg–Al–Zn alloys processed by high-pressure torsion. J. Mater. Sci. 2013;48:4661-4670.
[32] Xu C, Furukawa M, Horita Z, Langdon TG. The evolution of homogeneity and grain refinement during equal-channel angular pressing: A model for grain refinement in ECAP. Mater. Sci. Eng. A. 2005;398:66-76.
[33] Xu C, Langdon TG. The development of hardness homogeneity in aluminum and an aluminum alloy processed by ECAP. J. Mater. Sci. 2007;42:1542-1550.
[34] Wongsa-Ngam J, Kawasaki M, Langdon TG. The development of hardness homogeneity in a Cu–Zr alloy processed by equal-channel angular pressing. Mater. Sci. Eng. A. 2012;556:526-532.
[35] Wu Y, Baker I. An experimental study of equal channel angular extrusion. Scr. Mater. 1997;37:437-442.
[36] Kim HS, Hong SI, Seo MH. Effects of strain hardenability and strain-rate sensitivity on the plastic flow and deformation homogeneity during equal channel angular pressing. J. Mater. Res. 2001;16:856-864.
[37] Qiao XG, Starink MJ, Gao N. Hardness inhomogeneity and local strengthening mechanisms of an Al1050 aluminium alloy after one pass of equal channel angular pressing. Mater. Sci. Eng. A. 2009;513:52-58.
[38] Xu C, Horita Z, Langdon TG. The evolution of homogeneity in processing by high-pressure torsion. Acta Mater. 2007;55:203-212.

[39] Kawasaki M, Alhajeri SN, Xu C, Langdon TG. The development of hardness homogeneity in pure aluminum and aluminum alloy disks processed by high-pressure torsion. Mater. Sci. Eng. A. 2011;529:345-351.
[40] Kawasaki M, Ahn B, Langdon TG. Microstructural evolution in a two-phase alloy processed by high-pressure torsion. Acta Mater. 2010;58:919-930.
[41] Zhang NX, Kawasaki M, Huang Y, Langdon TG. Microstructural evolution in two-phase alloys processed by high-pressure torsion. J. Mater. Sci. 2013;48:4582-4591.
[42] Figueiredo RB, Langdon TG. Development of structural heterogeneities in a magnesium alloy processed by high-pressure torsion. Mater. Sci. Eng. A. 2011;528:4500-4506.
[43] Kawasaki M, Figueiredo RB, Langdon TG. An investigation of hardness homogeneity throughout disks processed by high-pressure torsion. Acta Mater. 2011;59:308-316.
[44] Kawasaki M, Figueiredo RB, Langdon TG. Twenty-five years of severe plastic deformation: recent developments in evaluating the degree of homogeneity through the thickness of disks processed by high-pressure torsion. J. Mater. Sci. 2012;47:7719-7725.
[45] Panda S, Toth LS, Fundenberger JJ, Perroud O, Guyon J, Zou J, Grosdidier T. Analysis of heterogeneities in strain and microstructure in aluminum alloy and magnesium processed by high-pressure torsion. Mater. Charact. 2017;123:159-165.
[46] Hussain M, Rao PN, Singh D, Jayaganthan R, Singh S. Comparative study of Microstructure and Mechanical properties of Al 6063 alloy Processed by Multi axial forging at 77K and Cryorolling. Procedia Eng. 2014;75:129-133.
[47] Cherukuri B, Srinivasan R. Properties of AA6061 processed by multi-axial compressions/forging (MAC/F). Mater. Manuf. Process. 2006;21:519-525.
[48] Magalhães DCC, Pratti AL, Kliauga AM, Rubert JB, Ferrante M, Sordi VL. Numerical simulation of cryogenic cyclic closed-die forging of Cu: hardness distribution, strain maps and microstructural stability. Mater. Res. Technol. 2018;8:333-343.

[49] Huang H, Zhang J. Microstructure and mechanical properties of AZ31 magnesium alloy processed by multi-directional forging at different temperatures. Mater. Sci. Eng. A. 2016;674:52-58.
[50] Flausino PCA, Nassif MEL, Bubani FC, Pereira PHR, Aguilar MTP, Cetlin PR. Influence of Strain Amplitude on the Microstructural Evolution and Flow Properties of Copper Processed by Multidirectional Forging. Adv. Eng. Mater. 2020;22:1-13.
[51] Yang Y, Mao Q, Zhao Y. Improving the combination of electrical conductivity and tensile strength of Al 1070 by rotary swaging deformation. Results Phys. 2019; 13:102235-102236.
[52] Hu H. Texture of Metals. Texture Stress Microsctruct. 1974;1:233-258.
[53] Pereira PHR, Wang YC, Huang Y, Langdon TG. Influence of grain size on the flow properties of an Al-Mg-Sc alloy over seven orders of magnitude of strain rate. Mater. Sci. Eng. A. 2017;685:367-376.
[54] Cao Y, Ni S, Liao X, Song M, Zhu Y. Structural evolutions of metallic materials processed by severe plastic deformation. Mater. Sci. Eng. R Rep. 2018;133:1-59.

4 CONCLUSÕES

A metodologia criada para o processamento por MDF confinado é eficiente para obter as curvas tensão x deformação durante o processamento, sem os problemas existentes no processamento livre e elimina a necessidade de usinagem entre as compressões.

A microestrutura obtida com o MDF confinado, após a deformação total de 0,9, adotando a amplitude de deformação de 0,075 em cada passe, é similar à obtida para o processamento sem o confinamento.

O processamento por MDF livre promove distorções na amostra e consequente heterogeneidade de microdureza. A amostra assume geometria romboédrica e apresenta maiores valores de microdureza na diagonal menor.

A usinagem entre os passes de MDF elimina as distorções geométricas e a distribuição desigual de microdureza entre as diagonais do prisma.

As medidas de microdureza, as simulações numéricas e as análises microestruturais indicam que a região central, das amostras processadas de forma livre com usinagem entre os passes e as amostras processadas em regime confinado, apresentam maiores deformações quando comparado com as regiões mais próximas às faces da amostra.

A remoção de material na usinagem após cada passe remove partes menos deformadas da amostra, o que reduz a heterogeneidade de deformação após a usinagem. As amostras usinadas após cada compressão apresentam menor heterogeneidade que as amostras processadas em regime confinado.

A evolução microestrutural para ambas as metodologias é similar. A região central da amostra processada por MDF confinado apresenta grãos mais refinados e mais próximos de equiaxiais quando comparados com a região lateral e quinas da amostra.

O processamento por MDF confinado é mais atrativo que as demais metodologias, pois: é simples, rápido, elimina a necessidade de usinagem entre as compressões, logo, é mais barato, e segue o mesmo caminho de deformação que o processamento livre e mantem o estado triplo de deformação.

5 SUGESTÕES PARA TRABALHOS FUTUROS

Realizar estudos com maior amplitude de deformação a fim de observar a diferença de heterogeneidade entre as metodologias adotadas.

Comparar os resultados obtidos com as metodologias que adotam estado plano de deformação.

Realizar ensaios de tração e compressão nas três diferentes direções, das amostras estudadas, com o objetivo de avaliar a anisotropia inerente ao processamento.

Executar o mesmo estudo em ligas de Alumínio para avaliar o efeito dos elementos de liga na distribuição de deformação e a evolução do comportamento mecânico e microestrutural.